Analysis of the air pollution climate of a central urban roadside supersite

Kamara, Adams A.; Harrison, Roy M.

DOI:
10.1016/j.atmosenv.2021.118479

Document Version
Peer reviewed version

Citation for published version (Harvard):
Kamara, AA & Harrison, RM 2021, 'Analysis of the air pollution climate of a central urban roadside supersite: London, Marylebone Road', *Atmospheric Environment*, vol. 258, 118479.
https://doi.org/10.1016/j.atmosenv.2021.118479

Analysis of the Air Pollution Climate of a Central Urban Roadside Supersite: London, Marylebone Road

Adams A. Kamara and Roy M. Harrison*†

School of Geography, Earth and Environmental Sciences
University of Birmingham
Edgbaston, Birmingham B15 2TT
United Kingdom

* To whom correspondence should be addressed (Email: r.m.harrison@bham.ac.uk)

†Also at: Department of Environmental Sciences / Center of Excellence in Environmental Studies, King Abdulaziz University, PO Box 80203, Jeddah, 21589, Saudi Arabia

ABSTRACT. The London Marylebone Road monitoring site is a roadside supersite adjacent to a highway carrying 80-90,000 vehicles per day on six lanes in a street canyon. Data from the Automatic Urban and Rural Network (AURN), Black Carbon Network, Automatic Hydrocarbon Network, Heavy Metal Network, Particle Size and Number and Particle Composition Network covering the period from 2009-2018 were analysed to determine short-term (diurnal, weekly and seasonal) and long-term variations and geographic source attribution. The contribution of roadside emissions relative to background sites (roadside increment) to the pollution climate was also investigated. The long-term trend analysis shows significant decline in regulated pollutants such as the particulate matter fractions (-4.0%; -3.93%/yr for $PM_{2.5}$ and PM_{10} respectively) and gas phase pollutants associated with vehicular emissions (-5.5%; -1.22% and -2.1%/yr for CO, NO_x and NO_2 respectively), although concentrations of SO_2 and O_3 have remained relatively constant over the years. Equivalent Black carbon (eBC) and total particle number count have also declined over the years whereas the heavy metals show mixed results (only Cu, Ni and V shows significant downward trends). The inorganic ionic components of the PM_{10} fraction, elemental (EC) and organic carbon (OC) and the volatile organic compounds all generally show declining trends over the period. Assessment of the diurnal variations shows elevated concentrations of the particulate matter fractions, the nitrogen oxides, CO and SO_2 at periods corresponding to the traffic rush hours, whereas O_3 peaked in the afternoon when there is less titration due to lower NO concentrations. The diurnal pattern of eBC and Total Particle Number Count are similar to NO_x and show strong traffic influence. Cl, Mg, K and Na levels show no systematic pattern throughout, with their presence likely controlled by meteorological conditions, and Ca showing high concentrations in the afternoon because of resuspension of deposited dust resulting from turbulence created by vehicular movement, and eroded road-surface material. Ammonium and nitrate show their lowest concentrations during the day when the temperature is high, probably reflective of their semi-volatile nature, with sulphate producing a peak around mid-day. The VOCs, with the exception of ethane, give the bimodal peaks typical of traffic related emission in the diurnal plots and their

pattern is more similar to CO than the other traffic emitted gaseous pollutants. Ethane is associated with leakages from gas supply pipes. The weekday plots show weekday (Monday – Friday) increases in traffic-related pollutants and a decline over the weekends due to lower traffic volumes, with the reverse observed for O_3. K and the marine aerosol components show relatively similar concentrations on all days of the week, while Ca, NH_4^+, NO_3^- and SO_4^{2-} all show a weekday maximum and decline over the weekend. The pollutants show seasonal variations; O_3 shows a springtime maximum, with the traffic-emitted pollutants (NO, NO_x, CO, EC, OC etc) giving a winter maximum due to increase in emission, lower mixing depth and poor dispersion. Particulate matter fractions and total particle count show lower concentrations in summertime reflective of the semi-volatile nature of some components. Ca shows less seasonal variability, with marine aerosol components showing a maximum winter concentration driven by higher wind speed conditions. NH_4^+, NO_3^- and SO_4^{2-} show lowest levels in summer and maximum springtime concentrations. The traffic-related VOCs show a summertime minimum and wintertime maximum, while isoprene shows increased concentrations during summertime. The street canyon circulation causes the sampling of North London air on northerly winds, but enhanced traffic pollution when winds have a southerly component. There is a sizeable roadside increment above the local background for both exhaust (particulate matter mass fractions, particle number and eBC) and non-exhaust emissions (heavy metals). However, roadside increments of inorganic species, which include Ca, marine aerosol components and the secondary particulate matter components, are not significant, indicating that they are mainly controlled by regional transport of the pollutants. Polar plots show strong local contributions for the regulated gas phase pollutants and the carbon components (EC and OC), with O_3 concentrations enhanced mainly from the northerly direction. The long-range contribution from mainland Europe to the particulate matter fractions is significant and occurs mainly as secondary aerosol. Ratios of OC/EC in particles have shown a steady increase due to a more rapid reduction of EC than OC.

Keywords: Air quality; trends, particulate matter; gaseous pollutants; roadside site; traffic pollution.

INTRODUCTION

London is the largest and most populated city in the UK and has a history of severe pollution events such as the notorious 1952 London smog that precipitated an increased awareness of air quality issues within the city. Investigating the trends, seasonality and cyclic patterns exhibited by air pollutants gives insights into their sources and properties, and is important for health considerations and policy development. Bigi and Harrison (2010) analysed 13 years of hourly data from a central urban background site in London for particulate matter and gas phase pollutants in terms of long-term trends, annual, weekly and diurnal cycles. The analysis showed generally declining trends for all the pollutants considered, with the exception of O_3 which exhibited a steady increase over the period. Clear seasonal variations were observed, with CO, NO, NO_2 and SO_2 showing a summer and winter maximum and a pattern associated with traffic emissions (for CO, NO and NO_2). O_3 showed a maximum in May and a minimum in winter, and the particle number count was at a minimum in August and a maximum in winter. Colette et al. (2011) investigated air quality trends in Europe over the past decade by looking at pollutants such as NO_2, O_3 and PM_{10} from urban background, suburban background and rural background stations. They observed a general decline in NO_2 for the majority of the monitoring stations, with a slight increase of O_3 observed (especially at urban sites) due to a decrease in NO_x emissions. PM_{10} levels declined over the decade in UK and Germany. Analysis of 18 years of data from Fresno (California) using time series and multiple linear regression models showed that the concentrations of NO_x, EC and ammonium nitrate had halved since 2000, but the $PM_{2.5}$ levels had not declined significantly (de Foy and Schauer, 2019). Similarly, in Los Angeles, an assessment of the effectiveness of regulations to reduce tail pipe emission was undertaken by investigating the trend in $PM_{2.5}$ mass concentration and chemical species concentrations for the period 2005 – 2015 (Altuwayjiri et al., 2021). The study reported an overall significant downward trend in mass concentration of EC and OC (major contributors to the $PM_{2.5}$ mass concentration). Data from 18 sites for the period 1999-2016 analysed for Seoul also showed a decrease in the long-term measurements of PM_{10} due to a reduction in the local source

contribution, and an increase in O_3 from local secondary production, with NO_2 and SO_2 not showing significant trends (Seo et al., 2018). This study also looked at short-term variability in pollutant concentrations, and was able to associate high PM_{10} and primary gaseous pollutant concentrations with migratory high-pressure systems that enhance regional transport and local accumulation during warmer periods.

This study examined data generated by different monitoring networks at the roadside London, Marylebone Road supersite, one of the most investigated roadside locations in Europe, with data from the North Kensington and the Westminster background sites utilised as required for comparison. Changes in the short and long-term trends of regulated pollutants, geographic source apportionment and roadside contribution increments were investigated. A similar analysis was also conducted for unregulated pollutant metrics (i.e. eBC, heavy metals, hydrocarbon and particle numbers). The results are consider as likely to be representative of heavily trafficked roadside locations across Europe, as over the relevant period, the UK was subject to EU Directives which applied also across many other countries in the region. This is especially true of vehicle emission standards which are applied to vehicles across Europe, even outside of the EU. Consequently, although there will be differences due to local source emissions and differing meteorology, there are broadly similar air pollution climates across Europe, especially in relation to road vehicle emissions.

METHODOLOGY

Marylebone Road is an important thoroughfare in central London. It runs east to west from the Euston Road at Regent's Park, to the A40 Westway at Paddington. The road, which has three lanes in both directions, is part of the London Inner Ring Road and as such forms part of the boundary of the zone within which the London congestion charge applies. As part of the Ring Road, it is a feeder route to the A40 (and hence the M40 motorway to the west) and the A5 and M1

motorway (to the north). Air sampling equipment is housed in a large kerbside cabin on the sidewalk of this busy central London street canyon. The adjacent six-lane highway carries around 80 000 vehicles per day. The highway is relatively straight and at this point runs almost due east – west (angle 80º from north). The buildings on either side of the highway are around six storeys in height, giving a street canyon aspect ratio of approximately 1:1 (Harrison et al., 2019).

- Data for this study were downloaded from the Automatic Urban and Rural Network for the regulated pollutants (gas phase and particulate matter), as well as for heavy metals, black carbon, particle number size distributions and hydrocarbons from the respective networks. The heavy metals data are based on an integrated 1-month period sampling of the PM_{10} fraction, while the other parameters are measured automatically and recorded over hourly periods. Quality assurance and quality control procedures follow the standards for the Automatic Urban and Rural Network (AURN) instruments, including regular span and zero checks, and every six months full servicing and an inter-calibration audit (https://uk-air.defra.gov.uk). Details of the instruments appear in Table S1. Data recovery is high (mostly >80%) for the hourly measurements especially for the regulated pollutants, not requiring any adjustments. For annual averages, as in the calculation of roadside increments, only periods with data availability at both locations are included.

The data were analysed mostly using the Openair package in the R software; see Carslaw (2015) for details of the analysis procedures. Long-term variability in measured concentrations of different pollutants were investigated using the Theil-Sen function, whereas the relative shorter time variations (diurnal, weekdays and monthly) used the Time Variation functions. Polar plots are used to identify geographical sources of pollutant origins. Roadside increments were investigated by subtracting the value for background location measurement from that of the London Marylebone Road (LMR) monitoring station measurement. The London North Kensington (LNK) station is use

as the background site for the estimation of the roadside increment for the particulate matter fractions, equivalent black carbon and the inorganic species whereas the London Westminster (LW) background site is use for the heavy metals estimation. The term "background site" is used to describe sampling locations where the pollution level is not influenced significantly by any single source or street, but rather by the integrated contribution from all sources upwind of the station. The surroundings of the LNK site are mainly residential with the closest road being usually quiet and no major highway in the vicinity. The nearest road to the LW site is about 17 metres away, and the surrounding area has mixed commercial and residential use."

Using a median wind speed, the typical atmospheric transport time from the background sites to the LMR site is 19 minutes. This is insufficient to justify any time shift in hourly mean data.

RESULTS AND DISCUSSION

Long-Term Trends in Pollutant Concentrations

Investigating long-term trends in pollutant concentrations is an asset in evaluating the effectiveness of control measures put in place for given pollutants. Monitoring of regulated pollutants and other pollutants of interest has taken place for a long time at the London Marylebone Road site leading to the accumulation of a huge dataset, suitable for such investigation.

Over the period 2009 – 2018 a significant decrease in the levels of the different particulate matter fractions, the nitrogen oxides (NO_x and NO_2) and carbon monoxide (Table 1) was observed. CO exhibits the highest rate of decline followed by the PM fractions and then the nitrogen oxides. The levels of O_3 and SO_2 have remained relatively constant, as they show an overall insignificant increase and decrease in trend respectively. At the London Marylebone Road, SO_2 arises mainly from road traffic. Low emissions of SO_2 from the transport sector is because of the introduction of low sulphur content (<50 ppb) diesel and petrol introduced in 1999 and 2001 respectively, with an even lower sulphur content fuel of <10 ppb few years later (Boulter and Latham, 2009). The

reduction in motor fuel sulphur to "zero sulphur" levels (<10ppm S) occurred in 2007, which is why concentrations and the traffic increment have remained low and fairly constant since. Road transport is one of the key emitters of air pollutants in urban areas, and this sector has been regulated for tail pipe emissions since the early 1990s by the Euro emission standards. According to Matthaios et al. (2019), the widespread use of the three-way catalyst in gasoline vehicles has brought about significant reduction in tail pipe emissions. Many diesel vehicles were fitted with an oxidation catalyst to meet the Euro 3 standard, introduced in 2000 leading to oxidation of CO and hydrocarbons but also to oxidation of NO leading to an increase in NO_2 emissions, corrected subsequently by a variety of technologies. These emission standards, introduced from 1992 onwards, applied only to new vehicles, so changes in air quality occur only gradually as new technology vehicles enter the fleet. Studies to determine the effectiveness of control measures to reduce exhaust emissions in London are available. Font and Fuller (2016) investigated 65 roadside monitoring sites in London for the period 2005 – 2009 and 2010 – 2014. The study generally showed a significant downward trend in roadside $PM_{2.5}$ for most of the sites with a mixed result for PM_{10}, but with most of the sites closer to the city centre showing a downward trend in PM attributed to use of diesel particle filters. The upward trends observed for PM_{10} in some of the sites is linked to an increase in the coarse particulate fraction (largely non-exhaust emissions). The study further reported an increase in NO_2 and NO_x concentration during 2005 – 2009 and attributed this to the increased proportion of light duty diesel vehicles. The decrease in levels of NO_x at most of the roadside sites between 2010 – 2014 was concluded to be the result of reduction in vehicle fleet number, and the introduction of the London Low Emission Zone, applying at that time to heavy duty vehicles. The reduction in roadside increment of PM levels, which is associated with the use of Diesel Particle Filters (DPF) from Euro 5, is also reported by Harrison and Beddows (2017), in a paired site study of London Marylebone Road and London North Kensington (2009 – 2015), a period during which no significant change in traffic flow and vehicle types was observed. The more stringent measures introduced by the Euro 6 standard (from 2014 with subsequent strengthening)

and the London Ultra-low Emission Zone from 2019 will have led to further reductions in NO_x emissions.

The instances of exceedances of European Union air quality standards are indicated in Supplementary Table S2. From 2012 to date, PM_{10} has not exceeded the 24 hrs mean Limit Value of 50 µg/m^3 (not to be exceeded more than 35 times per year) set for the protection of human health, with the number of exceedances per year decreasing over time. It has also stayed below the annual mean Limit Value for the past ten years, as is the case for $PM_{2.5}$ (the mean annual $PM_{2.5}$ concentration is below 25 µg/m^3 for the period 2009-2018). The levels of gas phase pollutants and particulate matter concentrations have been reported to be in decline across Europe for several years, with the reduction assumed to be the result of implementing abatement strategies and the introduction of the Integrated Pollution Prevention and Control (IPPC) directive (Cusack et al., 2012). Similarly, Sicard et al. (2021) in an investigation of the air quality status of European cities for the period 2000 – 2017, reported a significant decline in the emission of all primary pollutants at national level, even though the population exposures for some pollutants were found to be high in some cases i.e. exceeding limits set by EU Directives. On the other hand, for NO_2, the 200 µg/m^3 one-hour limit that should not be exceeded more than 18 times a year was exceeded for the entire period, with the least exceedance number of 31 times recorded in 2018. The annual mean limit of 40 µg/m^3 was also exceeded throughout this period. For O_3, the 8 hr mean limit of 100 µg/m^3 was not exceeded throughout the period under consideration. This is expected as there will be sufficient NO present from traffic emissions to suppress O_3 concentrations at this location.

There is a steady downward trend exhibited in the monthly mean NO_2 and CO concentrations throughout the period. The highest monthly levels for NO_2 were measured in 2009 (>120 µg/m^3), and these were <100 µg/m^3 by 2018. CO also had its highest monthly mean concentration of 0.9 mg/m^3 recorded in 2009. For NO_x, even though the lowest peaks (monthly average) occurred in

most recent times, the highest monthly concentrations occurred during the period 2012-2016. The particulate matter fractions ($PM_{2.5}$, PM_{10} and PM_{coarse}) like NO_2, show a steady decline, with the maximum monthly peaks occurring during 2011-2012. The maximum monthly mean concentrations for the PM fractions are 35 μg/m^3, 52 μg/m^3 and 18 μg/m^3 for $PM_{2.5}$, PM_{10} and PM_c respectively. There was a relatively constant level of O_3 and SO_2 concentrations from one year to the next during this period. For O_3, the maximum monthly peak concentrations >30 μg/m^3 have occurred since 2010 and are still observed for measurements as recently as 2018. SO_2 on the other hand showed maximum monthly peaks (≈11 μg/m^3) between 2014-2016 and is declining in the most recent measurements. The downward trend shown by the pollutants based on real time measurements is in line with the National Atmospheric Emissions Inventory in which there have been significant declines in emissions over the years, due to measures which reduced or eliminated the sources of such emissions (Figure S1). However, for most of these pollutants, the decline is either slowing down or has levelled off. For instance, since 2010 the decline in the oxides of nitrogen and SO_2 have slowed down (appearing to level off from 2020) while those of the regulated particulate matter fractions had started levelling off by 2015 (Defra, 2019).

The long-term trend for other pollutants has also been investigated (Table S3). For black carbon (BC), there has been a steady decline in the concentration of BC at an overall rate of 12.44%/year ($p < 0.001$). An average maximum concentration of 8 μg/m^3 was observed in 2014, with monthly average concentrations generally below 4 μg/m^3 measured in 2018 (i.e. decreasing by a factor of more than two). Trends in carbonaceous aerosol components across the UK are examined in more detail elsewhere (Jafar and Harrison, 2020). Total number particle count (TNC) shows a statistically significant ($p < 0.001$) downward trend in monthly mean concentration for the period 2011-2018. The average monthly total particle count was ≈ 65,000 count cm^{-3} in 2011 and has reduced to below 30,000 count cm^{-3} in 2018. The trends for the heavy metals for the period 2011-2018 give mixed results. Metals such as Cu (-3.59%/yr, $p < 0.05$), Pb (-2.92%/yr, $p < 0.05$), Ni (-

5.33%/yr, $p < 0.001$) and V (-7.21%/yr) show significant downward trends, whereas As has increased at a rate of 3.91%/yr ($p < 0.05$). The upward trend exhibited by arsenic is possibly due to increased emissions arising from domestic combustion of coal and treated wood for which data are highly uncertain. Fe, Mn and Zn have shown an upward trend, although such increases are not statistically significant, with Cd, Co, Cr and Se also showing a non-significant downward trend. Goddard et al. (2019) also reported similar long-term trends (based on off-line ICP-MS analysis) of metals at UK sites and attributed a recent increase in Mn to an increase in biomass fuel burning. Fe is the most abundant metal due to emissions of brake wear particles from road traffic (Gietl et al., 2010). The inorganic ionic components of the PM_{10} fraction show declining trends in most cases. Sodium and chloride ions are associated with marine aerosol and show a significant declining trend ($p < 0.001$) at similar rates i.e. at an overall rate of -7.77%/yr and -7.62%/yr respectively. The marked downward trend in sea salt component concentrations is probably explained by a decreased average speed of south-westerly winds, which declined by 1.99% per year between 2011 and 2018, as the generation of sea salt is strongly wind speed dependent. An alternative possibility is a reduced use of deicing salt, but we have been unable to obtain data to test the latter hypothesis. Ca and to some extent K ions have declined over the period, but the reasons are unclear. A reduction in the biomass burning source seems unlikely as concentrations of Brown Carbon at this site have increased (Jafar and Harrison, 2020). Mg is the only element that shows some semblance of an increasing trend even though it is not significant. The anthropogenic secondary aerosol components (ammonium, nitrate and sulphate) all show downward trends, and this decline will account in part for the decline in the particulate matter concentrations. While NH_4^+ shows an almost constant level and non-significant change, NO_3^- and SO_4^{2-} showed a significant downward trend ($p < 0.001$) at an overall rate of -7.91%/yr and -10.98%/yr respectively. These trends are also seen in those of the precursor molecules (NO_x and SO_2 respectively). However, the rate of decrease of NO_x (-2.17%/yr) and SO_2 (-2.67%/yr) are significantly lower than those of the secondary products, which are 7.91%/year and 10.98%/year for nitrate and sulphate respectively, for the period under

investigation. The decrease in the concentrations of the primary pollutants are in line with the reductions observed in the emissions of the pollutants as illustrated by the National Atmospheric Emissions Inventory (Figure S1). It was reported that between 2002 to 2004, regional background levels of secondary inorganic aerosol accounted for 88% and 92% of nitrate and sulphate respectively in Central London (Young et al., 2015). Therefore, the higher rate of decline of secondary aerosol components may be the combined outcome of a decline in long-range transport of secondary aerosol and a decline in the local emissions of the precursor molecules, but predominantly the former. Volatile Organic Compounds (VOCs) which are emitted from solvent use, consumer products, transport (combustion and evaporation) and leakages from gas pipes in urban areas showed a declining trend. With the exception of isoprene and ethane that showed a non-significant downward trend i.e., levels being relatively constant, the other nine VOCs show significant downward trends. 1,3-Butadiene, which is one of the VOCs with an air quality guideline in the UK showed the highest rate of decline at -12.59%/yr. Both 1,3-butadiene and benzene have annual averages below the limits stated in the National Air Quality Objectives of 2.25 $\mu g/m^3$ and 5 $\mu g/m^3$ respectively.

At the London, Marylebone Road (also for the background site at North Kensington), there is a significant decline in both Elemental Carbon (EC) and Organic Carbon (OC) for the period 2011-2018 at an overall rate of -7.54%/yr ($p < 0.001$) and -3.52%/yr ($p < 0.001$) respectively. For EC, the monthly average was ≈ 9 $\mu g/m^3$ in 2010 which reduced to a value of 2 $\mu g/m^3$ in 2018, whereas OC showed a monthly peak value of 9.8 $\mu g/m^3$ in 2011 which declined to 4.5 $\mu g/m^3$ at the start of 2018 (however it rose to ≈ 7 $\mu g/m^3$ later in the year). The OC/EC ratio, however, exhibited a significant upward trend at a rate of 8.77%/yr for the same period (rising from 0.5 to 2.9 by 2018). The yearly average OC/EC ratio is 1.2-2.4 at the site (Table S4). With the exception of 2018 with the highest ratio of 2.4, all the other years give values less than 2. Several studies have utilized the value of the OC/EC ratio to determine the sources contributing carbonaceous components to particulate matter

303 pollution. A ratio of 1.1 has been attributed to a contribution mainly of fossil fuel combustion to EC
304 and OC (i.e. primary emissions), whereas a ratio of up to 2.8 or more is because of a contribution of
305 secondary organic aerosol formation to OC (Zhang et al., 2009; Mbengue et al., 2018). The OC/EC
306 ratio values for the period under investigation for the Marylebone Road data indicates even though
307 primary emissions may have been the major contributor to carbonaceous emissions, there has been
308 a gradual shift to SOA being a major component of the OC fraction. This SOA may be from aged
309 materials transported over long distance to the monitoring station. However, such interpretations
310 risk being over-simplistic and the more likely explanation is an increased OC/EC ratio in vehicle
311 emissions due to the increasing use of diesel particle filters which remove involatile EC more
312 effectively than OC, much of which is semi-volatile (Beddows and Harrison, 2018; Alam et al,
313 2019).
314
315 **Diurnal, Weekday and Seasonal Variations**
316 Figure 1 gives the time series plots for some of the regulated pollutants with the left, middle and
317 right panels showing diurnal, seasonal and weekday variations in pollutant concentrations
318 (normalised) respectively. The level of the pollutants on any given day shows a strong traffic
319 influence i.e. a bimodal diurnal distribution corresponding to the early and late traffic rush hours
320 (Kendrick et al., 2015). The concentrations of the nitrogen oxides, PM fractions, CO and SO_2 all
321 give maximum concentrations during the period of the traffic rush hours. There are two visible
322 peaks for each of these pollutants corresponding to the early traffic rush hours (08:00-10:00 hrs)
323 and the late rush hours (after 18:00 hrs). During these periods of the day, less dispersion of
324 pollutants from a stable weather condition (low wind and a lower mixing depth) may also enhance
325 concentrations. For CO, the evening peak has a higher amplitude than the early rush hour peak,
326 which contrasts with the other traffic related pollutants. The reason for this is uncertain, but may be
327 related to the relative amounts of gasoline vehicle traffic in the westbound and eastbound lanes.
328 Generally, there is a relatively high constant concentration of the traffic related pollutants during the

day, i.e. between the traffic peak hours, due to a continuous high vehicular volume flow at the London Marylebone Road, as the characteristic 'afternoon dip' observed at many sites during daytime is almost missing. On the other hand, O_3 levels are at a maximum during periods with least NO emissions, with limited O_3 titration reaction and vice-versa. The O_3 peaks before 06:00 hrs in the morning and at around 15:00 hrs in the afternoon. However, absolute concentrations of ozone at the roadside are expected to be low as there is a sufficient supply of nitrogen oxide from vehicle exhaust to attenuate the concentrations.

The diurnal plot for eBC shows a typical traffic dependence of the pollutant concentration (similar to the pattern exhibited by other traffic emission related pollutants discussed above), with maximum levels observed between 08:00 hr to 18:00 hr, indicating continuous vehicular movement throughout this period. eBC is a major component of $PM_{2.5}$ emanating from tail pipes of vehicles in urban areas. However, a relatively weak correlation ($R^2 = 0.24$) exists between the two variables at this site. This may be because of other potential source contributions to $PM_{2.5}$ to this location. There is significant contribution by secondary aerosol transported from mainland Europe to $PM_{2.5}$ concentrations in southern England during easterly or southeasterly wind conditions (Harrison et al., 2012a). To understand the correlation between BC and $PM_{2.5}$ at the site better, a plot of the two variables as a function of wind direction produces a feature that explains how wind conditions contribute to the BC levels and distinguishes it from the other sources of BC at the London, Marylebone Road site (Figure 2). This shows higher eBC concentrations are associated with higher $PM_{2.5}$ concentration in the south-westerly wind direction and this is where the street canyon vortex carries fresh vehicle emissions to the air sampler (Harrison et al., 2019). There is also such strong correlation in higher concentrations of the species during easterly wind conditions. The northerly winds direction shows a stronger relationship with lower concentrations. This observation of the source contribution of BC to the $PM_{2.5}$ size fraction is also the dominant feature discussed in relation to the polar plots presented later. The low BC/$PM_{2.5}$ ratios in northerly wind sectors are

355 reflective of background air composition in those sectors without appreciable influence of local
356 traffic emissions (see below).
357
358 The diurnal variations in the inorganic species show a less obvious traffic dependence of these
359 pollutants (top and bottom left panels of Figure S2). Ca shows maximum levels during the period
360 when there is intense vehicular movement. This may be the result of resuspension of mineral matter
361 deriving from deposited dusts due to turbulence caused by vehicular movement, and attrition of the
362 road surfacing material itself. These processes may tend to be most efficient around noon when the
363 road surface is most likely to be dry. The other elements (Cl, Mg, K and Na) remain approximately
364 constant during the day, with their amount likely to be controlled by meteorological conditions, as
365 they are most likely not of traffic origin. Na, Cl and Mg are usually from a marine origin, whereas
366 K is a signature element of biomass burning, but is also present in crustal material such as soil. The
367 nitrogen containing species (ammonium and nitrate) show a similar pattern with maximum
368 concentrations around 08:00 hrs in the morning, but show their least concentrations during the
369 afternoon period, most probably reflecting the semi-volatility of ammonium nitrate (Harrison et al.,
370 2012a). The sulphate ion on the other hand shows a maximum peak close to mid-day and low,
371 constant concentrations on either side of this peak (i.e. morning and afternoon to night periods). The
372 behaviour of these inorganic species shows little traffic influence upon their levels, but formation
373 and sink processes that may be dominant at a certain time of the day determine their measured
374 concentrations.
375
376 The top and bottom left panels of Figure 3 give the diurnal variation plots for the volatile organic
377 compounds (VOCs), which show the bimodal peaks indicative of traffic emissions for all the VOCs
378 with the exception of ethane. Ethane is a major component of natural gas and its main source in the
379 urban atmosphere can be from gas pipeline leakage, while the other VOCs are either combustion
380 products from vehicle exhaust or arising from fuel evaporation and solvent use (isoprene can also

be from biogenic sources). The VOCs diurnal patterns (with the exception of ethane) are similar to that of CO with the evening rush hour peak showing a greater amplitude than that of the morning rush hour peak, reflecting a common source in gasoline engine emissions. The mainly traffic related VOCs ethyne, propene, 1,3-butadiene and benzene show high concentrations in the morning and evening periods associated with the traffic rush hours i.e. periods of maximum traffic volume. However, toluene, ethylbenzene and o-xylene although showing strong traffic influences are also major emissions from solvent use, that can also give high concentration during daytime due to higher temperatures. Shin et al. (2013) also report instances of VOCs not associated with traffic emissions (exhaust gases and gasoline vapour) and others showing a diurnal pattern associated with traffic sources, stating that such observations make it difficult to assign the main emission source. Isoprene that is emitted by many species of trees and by traffic shows increasing levels moving through the day, with emissions responding to an increase in ambient temperature. Ethane has a unique diurnal variation which can be easily explained if a constant rate of gas leakage is assumed. The concentration will be higher in the morning with a low mixing depth and a reduction in concentration as the boundary layer deepens during the day.

This feature exhibited by ethane can be useful in assessing the emission and dispersion of the other VOCs and gas phase pollutants, with the absolute ethane concentrations used as a normalization factor (Figure S3) i.e. the normalization is done by dividing the hourly concentration of each pollutants by the corresponding hourly ethane concentration. The diurnal patterns of the VOCs, including isoprene, and CO after ethane normalisation are similar suggesting a common source and the probability of them emanating from the same source i.e. road traffic. The bimodal peaks associated with traffic influenced emissions are absent in these plots, and there is a delay in the time maximum levels are observed i.e. showing a distinct difference between the period of maximum emission and that of maximum concentration within the boundary layer.

Total particle number count (TNC) also produces a diurnal pattern associated with traffic emissions with a continuous traffic flow between 08:00 hrs and 20:00 hrs. There is the typical maximum value corresponding to the time of day with intense vehicular activities, and the diurnal plot is very similar to that of eBC (Figure S4). eBC is a good tracer for diesel combustion from traffic sources and a major contributor to particle number count (Reche et al., 2011; Harrison et al., 2019). In this study, the diurnal profile for both parameters is similar, depicting a traffic generated pollutant, and elevated levels of eBC are observed for the southerly wind direction, a condition in which the sampler receives freshly traffic-emitted pollutants.

The weekday plots give the variability of the pollutant during the weekdays (Monday to Friday) and the weekends (see top and bottom left panels in Figures 1 and 2). Pollutants such as the oxides of nitrogen, SO_2, CO, the regulated particulate matter fractions, BC and particle total number counts all give maximum values on the weekdays, and the lowest concentrations over the weekend. The pollutant levels are observed to start to increase at the start of the week, attain a relatively constant level, and start to decline as the weekend approaches. These patterns are similar to the traffic volume for London Marylebone Road, which is slightly higher on the weekdays than the weekend (Figure S5), with the traffic profile aligning with that of the traffic related pollutants. Ozone that usually shows lower concentrations with a high NO concentration shows an increased concentration towards the weekends and a decrease to attain minimum levels during the weekdays. The concentrations of the marine aerosol related species and potassium are relatively constant throughout the weekdays in contrast to Ca that shows a maximum during the week and declines over the weekend. NH_4^+, and SO_4^{2-} also exhibit a similar weekdays plot as that of Ca. With the exception of ethane, all the VOCs investigated give weekday plots similar to those of the traffic related pollutants. Ethane shows slightly increased levels in the atmosphere on weekdays relative to the weekend, possibly due to increasing usage of the gas in areas close to the monitoring station. The EC and OC give a similar weekdays pattern with levels higher during the week and a dramatic

433 decline approaching the weekend; this observation is indicative of a significant contribution of road
434 traffic emissions to EC and OC. However, the situation is reversed for the OC/EC ratio, with the
435 highest values recorded over the weekend, due to a greater decline in EC than OC.
436
437 There is a clear seasonal variability exhibited by the different pollutants investigated in this study.
438 The different seasons and the associated months are defined as follows: Winter (DJF), Spring
439 (MAM), Summer (JJA) and Autumn (SON). The United Kingdom is a net sink for some of these air
440 pollutants, so long-range transport of pollutant will influence the seasonal measurements and
441 patterns observed. For instance, ozone shows a springtime maximum in May (and a minimum in
442 November) similar to observations of the northern hemisphere background at Mace Head, a location
443 reflective of intercontinental and regional long-range transport of the pollutant to the UK (Derwent
444 et al., 2015). It has been suggested that elevated levels of O_3 in springtime and summertime may be
445 the result of photochemical reactions of the transported ozone precursor molecules that have
446 accumulated over the winter period (Cristofanelli and Bonasoni, 2009; Vingarzan, 2004). NO and
447 NO_x generally show seasonal fluctuations opposite to those of O_3 i.e. winter high and a springtime
448 to summer low. High winter concentrations may result from less mixing in a shallower boundary
449 layer during winter and increased emissions from heating of homes and car usage. NO_2 on the other
450 hand shows relatively small seasonal changes. The seasonal change in concentrations of particulate
451 matter is highly influenced by temperatures changes, as the highest values are observed during
452 cooler periods with the lowest measured between June and August when the temperatures are at
453 their highest. The low level of PM in summer is in part due to longer daylight hours and higher
454 temperatures causing vaporization of the semi-volatile components especially the ammonium
455 nitrate-rich aerosol (Harrison et al., 2012a). CO and SO_2 both exhibit seasonal patterns similar to
456 those of the particulate matter fractions. Primary pollutants with little seasonal variation in source
457 strength such as BC and NO_x (mainly from local traffic) show higher concentrations in winter due
458 to weaker atmospheric mixing and dispersion. The total particle counts of the PM size fractions

record their least concentrations during summer due to vaporization of volatile components with the maximum levels recorded during the cooler periods, as ambient concentrations are affected by ambient temperature (Charron and Harrison, 2003; Sabaliauskas et al., 2012) as well as atmospheric mixing. During winter, particle number concentrations tend to increase at traffic locations due to enhanced condensation of the hot tailpipe emission and new particle formation especially for particle fractions with diameter less than 50 nm (von Bismarck-Osten et al., 2013).

Cl, Mg and Na ions show a winter maximum and a summer minimum. High concentrations of Cl and Na in winter are due to average higher wind speed leading to increased marine aerosol in the atmosphere (Twigg et al., 2015; Abdalmogith and Harrison, 2006), and a contribution from road deicing salt is possible. Ca shows limited seasonal variability while K shows a summer minimum and a maximum concentration in December, probably related to biomass burning. NH_4^+, NO_3^- and SO_4^{2-} all show a maximum concentration in March and the least amount in summer. There is an increased nitrate concentration from summer to winter. This increase in concentration in winter can be explained as an increase in the formation of nitrate on aerosol particles and a longer lifetime of nitrate in winter than in the summer period, during which there is a high dry deposition velocity of HNO_3 (Fisseha et al., 2006). Frequent regional transport events from mainland Europe are also a common feature in the spring. Hui et al (2018) state that seasonal variability in VOC concentrations in the atmosphere depends on the changes in VOC sources, OH radicals and the atmospheric mixing state. High temperature, strong solar radiation and efficient atmospheric mixing (i.e. strong convection) during the summer enhances photochemical depletion of the VOCs, therefore favouring lower concentrations during this period. On the other hand, in the winter period, the atmospheric boundary layer is shallower; the temperature stratification is more stable leading to less dilution of the pollutants. All this leads to a lower photochemical consumption in the winter and maximum pollutant concentrations. Ethane, ethyne, propene, 1,3-butadiene and benzene all show a summer minimum and a winter maximum. The VOCs more associated with solvent use

485 (toluene, ethylbenzene and o-xylene), increase in concentration from February and attain their
486 maximum in November. Isoprene gives maximum concentrations in summer due to an increase in
487 both biogenic and evaporative emissions at higher temperatures. There is a strong seasonal change
488 exhibited by EC and OC. EC has a minimum value in April and a maximum value in September,
489 whereas OC shows its least levels during July and maximum in November. The seasonal pattern of
490 the OC/EC ratio has its highest value in March and its lowest value in September. Several studies in
491 Europe have indicated maximum EC and OC concentrations in winter and the minimum in summer
492 (Mbengue et al., 2018; Jones and Harrison, 2005). However, for this study, the maximum levels for
493 both components were recorded in autumn. The reasons are unclear.
494
495 **Roadside Increments**
496 The contributions of traffic emissions at the London, Marylebone Road site above background
497 pollutant concentrations have been investigated for particulate matter, BC and heavy metal
498 concentrations by subtraction of simultaneously measured concentrations from the London, North
499 Kensington background site, located in a residential area of central London (Bigi and Harrison,
500 2010). In estimating the roadside increments, it is assumed that the pollution level at the
501 background site is representative of urban background levels and this is not influenced significantly
502 by any single source in the surrounding area, but rather by the integrated contribution from all
503 sources upwind of the station. Therefore, the difference in the pollutant concentration at the
504 roadside and background sites should be solely influenced by traffic emissions. Pollution arising
505 from long-range transport influences both locations to a similar extent.
506
507 As expected, there is a higher concentration of particulate matter at the London, Marylebone Road
508 site relative to the background site at North Kensington for the period under investigation. The
509 average yearly increment ranges from 4.5-9.0 $\mu g/m^3$ for $PM_{2.5}$ and 9.9-16.7 $\mu g/m^3$ for PM_{10}, with
510 2014 giving the lowest yearly mean for both PM fractions (Table 2). This shows data for

511 comparison derived from the hourly continuous instrumental data, and from 24-h average data
512 derived from gravimetric determination of filters. The coarse fraction (PM_c) also showed a roadside
513 increment throughout with annual mean values between 4.2 and 9.7 $\mu g/m^3$ (daily data). These
514 increments in the different roadside size fractions can be related to roadside emissions consisting of
515 both exhaust and non-exhaust contributions (Thorpe and Harrison, 2008; Harrison et al, 2012b).
516 The year-to-year variability and apparently anomalous negative value in Table 2 (hourly data) may
517 be in part attributable to incomplete data recovery (see Table S5 for data recovery data).
518
519 Investigation of the long-term trend of the ΔPM_{10} shows a significant decline in the monthly mean
520 value for PM_{10} ($p < 0.001$) with a relatively constant trend exhibited for $\Delta PM_{2.5}$. The diurnal plot
521 for the roadside increment for both $PM_{2.5}$ and PM_{10} shows a higher increment between the period
522 08:00 hrs and 18:00 hrs corresponding to the period of the day with greater vehicular movement
523 (Figure S6). The weekday trend shows the usual higher levels on the weekdays with lowest levels
524 over the weekend as observed typically for traffic related pollutants. However, there is difference in
525 trend in the seasonal variation of $\Delta PM_{2.5}$ and ΔPM_{10}. $\Delta PM_{2.5}$ shows a downward trend from the
526 start of the year to its minimum value in spring (April) and then a rise to a maximum value in early
527 autumn (September). In the case of PM_{10}, the trough observed for $PM_{2.5}$ in April is completely
528 absent, but rather a rise in value from the start of the year to its first maximum in late spring (May)
529 and a second one in August are seen. The reasons are not fully clear and issues of incomplete data
530 recovery may contribute to the divergence in trends.
531
532 There is a significant decline in roadside increment for eBC at an overall rate of 13.48%/year ($p <$
533 0.001) at the Marylebone Road relative to the urban background site at North Kensington for the
534 period 2014-2019. A maximum monthly increment >6 $\mu g/m^3$ was recorded in 2014 and a minimum
535 monthly average of <2 $\mu g/m^3$ in 2019. The reduction in BC increment is consistent with the
536 reduction in diesel particle emissions which followed the introduction of diesel particle filters on

Euro 5 vehicles which first entered the market in 2009 (Beddows and Harrison, 2018). The diurnal, weekday and seasonal/monthly variation of the roadside BC increment are similar to those exhibited by $\Delta PM_{2.5}$, showing a strong exhaust emission contribution to the BC increment (Figure S7).

Roadside emissions of heavy metal species are mainly associated with non-exhaust emissions that derive from the wear of tyres (Zn) and brakes (Cu, Fe) or components of the road surfacing materials and surface dust (Ca, Al, Fe) with Mn attributed to biomass fuel burning by Goddard et al. (2019), although this seems unlikely to apply to the roadside increment. Figure 4 shows Fe as the major component for PM_{10} composition followed by Cu, Zn, Mn, Cr and Pb. This reflects the contributions of brake wear, tyre wear and road surface wear and/or re-suspended road dust.

The roadside increment of metals was investigated by subtracting average yearly metal concentrations from the London, Westminster background site from that of the London, Marylebone Road site for the period 2011-2018. The London, Westminster monitoring station is located within a self-contained housing in the car park of the mortuary and coroner's court. The nearest road is the B323 Horseferry Road approximately 17 metres north of the station. The surrounding area is mixed commercial and residential. Table 3 shows that there is a roadside increment at LMR of all the metals throughout the period under consideration with the exception of 2013-2015 which show a lower level of Pb along the road. The data show that there has not been significant decrease in the concentrations from 2011 to 2018, consistent with the lack of controls on non-exhaust sources.

There are very small roadside increments and decrements in the yearly average for the different inorganic species of the PM_{10} fraction for the period under investigation, i.e. 2011 to 2018 (Table S6) for which the North Kensington site was the background. Such observations illustrate minimal

local contributions to the pollutants but significant concentrations resulting from long-range transport of the pollutants. However, during winter there is some evidence for a higher concentration of Ca, Cl and Mg at the background site relative to the roadside possibly due to a greater usage of de-icing salts (Ca, Mg and Cl are components of de-icing salts). With the exception of Na with four (50%) out of the eight yearly average readings showing a decrement at the roadside, all the other inorganic species give roadside decrements in 62.5%-85.5% of the average yearly readings.

Vehicular activities contribute to elevated levels of both EC and OC at the Marylebone Road site (Table 4). Inspection of the yearly mean values show the yearly mean contribution of EC is declining (maximum increment of 5.89 μg/m^3 in 2011 and a value of 1.83 μg/m^3 by 2018). The yearly mean roadside increment for OC has decreased slowly throughout the period, consistent with control of diesel particles which contain a predominance of EC relative to OC.

Geographical Source Attribution of Air Pollutants

Urban street canyons have a tendency to have high levels of particulate pollution due to restricted dilution resulting from the geometry of such locations (von Bismarck-Osten et al., 2013). At the Marylebone Road site, pollutant levels are highest between the 225 and 270º (or southerly) wind sectors, during which time the sampler receives freshly traffic-emitted pollutants due to the street canyon vortex, and the northerly wind sector is associated with background air from North London (Harrison et al., 2019). The latter point is shown clearly by Figure 5, which plots PM_{10} measurements at Marylebone Road against those for North Kensington for northerly wind sectors, showing very similar concentrations.

A significant contribution of roadside emissions is shown by high concentrations of the nitrogen oxides at both low and high wind speeds (Figure 6). Marylebone Road is an urban street canyon and

589 the circulation of the air parcel within the street canyon can result in high pollutant concentrations at
590 high wind speeds especially during southerly and south-westerly wind events, as seen in Figure 6.
591 Wind directions are taken from London, Heathrow airport and represent directions above, rather
592 than within the canyon.
593
594 For the other gas phase pollutants (Figure S8), CO and SO_2 show a significant local source
595 contribution at low wind speeds, with appreciable levels also recorded at high wind speeds for wind
596 originating from the southerly direction. O_3 on the other hand shows higher concentrations during
597 high wind speeds from the north and north-east of the monitoring site, corresponding to low NO_x at
598 the site.
599
600 The PM_{10} and $PM_{2.5}$ fractions show both a local (w.s. < 2 m/s) and a long-range/regional
601 contribution from the easterly direction at high wind speed (Figure 7). In the UK, several studies
602 have identified long-range transport of fine particulate matter especially from the east (or south-
603 east) comprising air masses originating from continental Europe, with nitrate and sulphate
604 dominating the particle composition (Grange et al., 2016; Bigi and Harrison, 2010). The
605 contribution of PM_c to PM_{10} is greatest during high wind speeds, especially from the easterly and
606 westerly wind directions. This is possibly due to road dust resuspension when the wind direction is
607 parallel to the road.
608
609 The polar plots of the robust slope (Figure S9) of $PM_{2.5}/PM_{10}$ and PM_c/PM show clearly the
610 predominance of finer particles in the air masses advected from the easterly sector, often
611 attributable to mainland Europe. A similar plot for the $BC/PM_{2.5}$ slope (Figure 8) emphasises the
612 role of traffic on Marylebone Road as a source of $PM_{2.5}$.
613

All of the inorganic components show elevated concentrations at higher wind speed, which is usually associated with long-range transport of pollutants (Figure S10 and S11). However, some also show in addition to that, higher levels at wind speeds < 2 m/s, indicative of a local emission source contribution. Both Ca and K show elevated concentrations at wind speed ≤ 2 m/s. Local source emissions of Ca include road surface abrasion and resuspension of road surface dust particles. Both local and regional biomass combustion contribute to significant levels of K measured at the site (Harrison et al., 2012b). The components of marine aerosols all show elevated concentrations during high wind speeds. The south-west direction gives the highest concentrations for the chloride ions followed by the easterly direction; Na shows maximum concentrations from the southeast with the southwest quadrant also recording high concentration; the reasons are unclear, but may relate to aged marine aerosol from the southeast. The mass concentrations of Na^+ and Cl^- in fresh sea salt are 0.308 g/g and 0.554 g/g respectively (White, 2008), giving an Na^+/Cl^- ratio of 0.556. Figure S12 shows that this ratio is generally observed on strong winds from the south-westerly direction indicating a contribution of fresh sea salt, whereas the other directions show depleted levels of Cl^- (due to removal by chemical reaction) thereby giving higher ratios. Crilley et al (2017) conducted a source apportionment study at this same location using a combined positive matrix factorization (PMF) and conditional probability function (CPF) approach in which the chlorine level was used to assign two different marine aerosol types i.e. fresh and aged sea salt particles. The study indicated that marine aerosol originated from different wind directions with the south/southwest wind component accounting for the highest contribution of fresh sea salt during high wind speed conditions. The study also identified a significant contribution of marine aerosol originating from the coastline areas in the east, but with greater chlorine depletion.

There are also maximum concentrations for Mg from the east and southwesterly directions. The major components of the anthropogenic secondary inorganic particulate matter (NO_3^-, NH_4^+ and SO_4^{2-}) all show their highest concentrations emanating from the easterly directions indicating

mainland Europe as the dominant source of the pollutants (a similar plot is also observed for the North Kensington monitoring site). Nitrate, ammonium and sulphate also show some local contribution to elevated levels. These features exhibited by the species are similar to those of PM_{10} (and $PM_{2.5}$), as they are the major components of particulate matter recorded at this location. The atmospheric composition is hence strongly influenced by meteorology, with sea salt dominating air masses from the ocean and secondary inorganic aerosol dominating air masses coming from mainland Europe (Twigg et al., 2015). Figure 9 shows an important local primary source contribution (i.e. traffic emissions) for EC and OC concentrations recorded during lower wind speed conditions (<2 m/s). Elevated concentrations at high wind speed conditions in the southerly/southwesterly sector can be attributed to emissions within the street canyon. The elevated concentrations observed from the east and southeasterly directions, especially for OC, are probably due to long-range transport.

Particle number and size distribution

The long-term plot of total particle count from the condensation particle counter for the Marylebone Road site shows a statistically significant ($p < 0.001$) downward trend in monthly mean concentration for the period 2011-2018. The average monthly total particle count averaged ≈ 38,000 # cm^{-3} in 2011 and has reduced to around 11,000 # cm^{-3} in 2019 (Figure 10).

The diurnal and weekday variations (left and right panels respectively in Figure 11) show a typical traffic dependence of the total particle number i.e., the typical peaks corresponding to the time of day with intense vehicular activities. The number count is at its highest during the weekdays and declines over the weekends. There is also seasonal variability, with autumn to winter maxima and the least counts recorded during summer. During winter, particle number concentrations tend to increase at traffic locations due to enhanced condensation of the hot tailpipe emission and new

particle formation especially for particle fractions with diameter less than 50 nm (von Bismarck-Osten et al., 2013).

These features exhibited for the three different timescales are similar to those shown by both the PM_{10} and $PM_{2.5}$ mass concentration plots. However, a notable difference arises in the seasonal plots in which the time at which the maximum peaks is seen. For all three parameters, there are peaks for both spring and autumn seasons; however, for the particle number count, the highest peak occurs in autumn with the second highest in spring, whereas it is the reverse for PM_{10} and $PM_{2.5}$ concentrations. PM mass is more influenced by regional transport of particles than particle number due to the effects of coagulation and evaporation of traffic particles.

There is an increase of particle number count recorded during both low and high wind speed conditions between 100-270^{o} (Figure 12). In the southerly and southwesterly directions, high concentrations at low wind speed is reflective of direct emission from the road as the location of the monitor favours sampling of fresh materials in this direction. Recirculation of particles within the street canyon can account for elevated concentrations during heavy winds. In addition, a long-range transport effect is observed from the easterly and southeasterly directions. Wind coming from this direction has been identified to carry pollutants originating from continental Europe.

Figure 13 shows a lognormal particle size and number distribution for the average monthly measurement for the period 2010-2018, for particles within the size bins of 16-600 nm. The size distribution is typical of those reported previously for this site (Charron and Harrison, 2003; Jones et al., 2012; Harrison et al., 2019).

The distribution is dominated by ultrafine particles (<100 nm). This feature is common to the distribution curves shown in Figure S9 in the Supplementary Information for each of the years

691 under consideration (i.e., 2010-2018) with all the mode(s) in the Aitken range. The modal diameter
692 and curve shape have changed over the years, and a consistent trend is seen in the data (Figure S13).
693
694 **Comparison with other sampling sites**
695 Table 5 summarises literature that contains a number of studies of air sampling sites with long time
696 series of measurements. Similar studies have identified patterns in pollutant concentrations within
697 urban areas with regular cycles established. Local emissions and meteorological conditions are seen
698 to be key factors determining pollutant concentrations during given periods. Long-term trends in
699 concentration reflecting changing emissions have been identified.
700
701 **CONCLUSIONS**
702 All of these studies have identified traffic emissions as a major source of urban pollution. Even
703 though the studies were conducted in different regions, most pollutants showed a decline over time,
704 except O_3 which rose steadily. Wintertime was the most polluted season in these different urban
705 locations.
706
707 Broadly similar trends have been observed in this study of the Marylebone Road site, but it is
708 differentiated from the other studies outlined above by:
709 (i) many more variables/pollutants are investigated;
710 (ii) the location of the monitoring site is within a street canyon in the centre of London; and
711 (iii) the specific contribution of vehicular emissions is investigated through calculation of the
712 roadside increment.
713
714 The investigation of data from the various monitoring networks shows various processes controlling
715 the pollutant concentrations in the urban atmosphere of Central London. Strong policies and
716 appropriate emission technologies are responsible for the observed decline in the long-term trend

717 analysis of traffic related pollutants. Emission rates and meteorological conditions are also key in
718 accounting for the relatively short term (diurnal and weekday) and seasonal variations observed for
719 pollutant concentrations. The diurnal plots for the traffic related pollutants show peak
720 concentrations during periods when there are increased vehicular emissions, weaker mixing and
721 poor dispersion accounting for peak levels for pollutant concentrations during the time of the traffic
722 rush hours. The seasonal effect shows winter as generally the most polluted period, a condition
723 enhanced by increased emissions and poor dispersion conditions.
724
725 Road traffic emissions (exhaust and non-exhaust) are a major contributor to pollution of urban
726 areas and this is reflected in the roadside increment in particulate matter fractions, BC, EC and OC
727 and heavy metals. Several inorganic species (Ca and those associated with marine aerosol and
728 secondary particulate matter) show measured concentrations being controlled by meteorological
729 conditions, with several periods for which the background site measures greater concentrations.
730 Meteorology strongly influences the composition of the atmosphere at this location, wherein local
731 emissions (vehicular) strongly dominate for the nitrogen oxides, CO and SO_2 (and a part of PM),
732 hemispheric and regional transport are dominant for O_3, marine aerosol components and particulate
733 matter. The particulate matter (PM_{10} and $PM_{2.5}$) originate from continental Europe mainly as
734 secondary aerosol as is shown by the polar plots for NO_3^-, NH_4^+ and SO_4^{2-}.
735
736 The Marylebone Road site exceeds the Limit Values for NO_2, although it is worth noting that the
737 extent of these exceedances has been declining over the period under investigation. The annual and
738 24-hour concentrations of PM_{10} and $PM_{2.5}$ are however largely in compliance with the Limit
739 Values. These results are reflective of the effectiveness of control measures that have been
740 instituted in recent years, although much remains to be done for the protection of public health,
741 especially in relation to non-exhaust emissions of particles, and regional transported secondary
742 particles.

DATA AVAILABILITY

Data supporting this publication are openly available from the UBIRA eData repository at https://doi.org/10.25500/edata.bham.00000577

ACKNOWLEDGEMENTS

We would like to acknowledge the main sponsor, The Islamic Development Bank (Merit Scholarship Programme for High Technology for Ph.D. Study) for their financial and moral support towards the student's Ph.D. study. We also extend our appreciation to the University of Birmingham (International Recruitment) for facilitating a 30% tuition fee discount. Data for this study was obtained from the Department of Environment, Food and Rural Affairs (DEFRA) website and is gratefully acknowledged.

SUPPORTING INFORMATION

Supporting Information provides details of instrumentation, data capture, exceedance of threshold concentrations, OC/EC ratios, as well as further diurnal and polar plots.

CONFLICT OF INTERESTS

The authors declare no competing financial interest.

REFERENCES

Abdalmogith S.S., Harrison R.M., 2006. An analysis of spatial and temporal properties of daily sulfate, nitrate and chloride concentrations at UK urban and rural sites, J. Environ. Monit., 8, 691-699.

Alam, M.S., Zeraati-Rezaei, S., Xu, H., Harrison, R.M., 2019. Characterisation of gas and particulate phase organic emissions (C9-C37) from a diesel engine and the effect of abatement devices, Environ. Sci. Technol., 53, 11345-11352.

Altuwayjiri, A., Pirhadi, M., Taghvaee, S., Sioutas, C., 2021. Long-term trends in the contribution of PM2.5 sources to organic carbon (OC) in the Los Angeles basin and the effect of PM emission regulations. Faraday Discuss., 226, 74.

Beddows, D.C.S., Harrison, R.M., 2018. Identification of specific sources of airborne particles emitted from within a complex industrial (steelworks) site, Atmos. Environ., 183, 122-134.

Bigi, A., Harrison, R.M., 2010. Analysis of the air pollution climate at a central urban background site, Atmos. Environ., 44, 2004-2012.

Boulter, P.G., Latham, S., 2009. Emission factors 2009: Report 5 – a review of the effects of fuel properties on road vehicle emissions. Published Project Report PPR358, Department of Transport, Cleaner Fuels and Vehicles, https://assets.publishing.service.gov.uk/government/uploads/system/uploads/attachment_data/file/4251/report-5.pdf [last accessed 04/11/20].

Carslaw, D.C., 2015. The openair manual — open-source tools for analysing air pollution data. Manual for version 1.1-4, King's College London.

Charron A., Harrison, R.M., 2003. Primary Particle formation from vehicle emissions during exhaust dilution in the roadside atmosphere, Atmos. Environ., 37, 4109-4119.

Colette, A., Granier, C., Hodnebrog, Ø., Jakobs, H., Maurizi, A., Nyiri, A., Bessagnet, B., D'Angiola, A., D'Isidoro, M., Gauss, M., Meleux, F., Memmesheimer, M., Mieville, A., Rouil, L., Russo, F., Solberg, S., Stordal, F., Tampieri, F., 2011. Air quality trends in Europe over the past decade: a first multi-model assessment, Atmos. Chem. Phys., 11, 11657-11678.

Crilley, L.R., Lucarelli, F., Bloss, W.J., Harrison, R.M., Beddows, D.C., Calzolai, G., Nava, S., Valli, G., Bernardoni, V., Vecchi, R., 2017. Source apportionment of fine and coarse particles at a roadside and urban background site in London during the 2012 summer ClearfLo campaign. Environment Pollution, 220, 766 – 778.

Cristofanelli, P., Bonasini, P., 2009. Background ozone in the southern Europe and Mediterranean area: Influence of the transport process, Environ. Pollut., 157, 1399-1406.

Cusack, M., Alastuey, A., Perez, N., Pey, J., Querol, X., 2012. Trends of particulate matter ($PM_{2.5}$) and chemical composition at a regional background site in the Western Mediterranean over the last nine years (2002-2010), Atmos. Chem. Phys., 12, 8341-8357.

de Foy, B, Schauer, J.J., 2019. Changes in speciated $PM_{2.5}$ concentrations in Fresno, California, due to NO_x reductions and variations in diurnal emission profiles by day of week. Elem. Sci. Anth, 7, 45, https://doi.org/10.1525/elementa.384.

Defra, 2019. Defra National Statistics Release: Emission of air pollutants in the UK, 1970-2017, https://www.gov.uk/government/publications/emissions-of-air-pollutants/emissions-of-air-pollutants-in-the-uk-1970-to-2018-summary.

Derwent, R.G., Utembe, S.R., Jenkin, M.E., Shallcross, D.E., 2015. Tropospheric ozone production regions and the intercontinental origins of surface ozone over Europe, Atmos. Environ., 112, 216-224.

Faridi, S., Shamsipour, M., Krzyzanowski, M., Kunzli, N., Amini, H., Azimi, F., Malkawi, M., Momeniha, F., Gholampour, A., Hassanvand, M.S., Naddafi, L., 2018. Long-term trends and health impact of $PM_{2.5}$ and O_3 in Tehran, Iran, 2006-2015, Environ. Int., 114, 37-49.

Fisseha, R., Dommen, J., Gutzwiller, L., Weingartner, E., Gysel, M., Emmenegger, C., Kalberer, M., Baltensperger, U., 2006. Seasonal and diurnal characteristics of water soluble inorganic compounds in the gas and aerosol phase in the Zurich area, Atmos. Chem. Phys., 6, 1895-1904.

Font, A., Fuller, G.W., 2016. Did policies to abate atmospheric emissions from traffic have a positive effect in London?. Environmental Pollution, 218, 463 – 474.

Font, A., Guiseppin, L., Blangiardo, M., Ghersi, V., Fuller, G.W., 2019. A tale of two cities: is air pollution improving in Paris and London? Environment Pollution, 249, 1 – 12.

Gani, S., Bhandari, S., Seraj, S., Wang, D.S., Patel, K., Soni, P., Arub, Z., Habib, G., Ruiz, L.H., Apte, J.S., 2019. Submicron aerosol composition in the world's most polluted megacity: the Delhi Aerosol Supersite study. Atmospheric Chemistry and Physics, 19, 6843 – 6859.

Gietl, J.K., Lawrence, R., Thorpe, A.J., Harrison, R.M., 2010. Identification of brake wear particles and derivation of a quantitative tracer for brake dust at a major road, Atmos. Environ., 44, 141-146.

Goddard, S.L., Williams, K.R., Robins, C., Butterfield, D.M., Brown, R.J.C., 2019. Concentration trends of metals in ambient air in the UK: a review, Environ. Monit. Assess., 191, 683.

Grange, S.K., Lewis, A.C., Carslaw, D.C., 2016. Source apportionment advances using polar plots of bivariate correlation and regression statistics, Atmos. Environ., 145, 128-134.

Harrison, R.M., Beddows, D.C., 2017. Efficacy of Recent Emissions Controls on Road Vehicles in Europe and Implications for Public Health. *Sci Rep* **7,** 1152. https://doi.org/10.1038/s41598-017-01135-2.

Harrison, R.M., Beddows, D.C.S., Alam, M.S., Singh, A., Brean, J., Xu, R., Kotthaus, S., Grimmond, S., 2019. Interpretation of particle number size distributions measured across an urban area during the FASTER campaign, Atmos. Chem. Phys., 19, 39-55.

Harrison, R.M., Laxen, D., Moorcroft, S., Laxen, K., 2012a. Processes affecting concentrations of fine particulate matter ($PM_{2.5}$) in the UK atmosphere, Atmos. Environ., 46, 115-124.

Harrison, R.M., Beddows, D.C.S., Hu, L., Yin, J., 2012b. Comparison of methods for evaluation of wood smoke and estimation of UK ambient concentrations, Atmos. Chem. Phys., 12, 8271-8283.

Hui, L., Liu, X., Tan, Q., Feng, M., An, J., Qu, Y., Zhang, Y., Jiang, M., 2018. Characteristics, source apportionment and contribution of VOCs to ozone formation in Wuhan, Central China, Atmos. Environ., 192, 55-71.

Jafar, H.A., Harrison, R.M., 2020. Spatial and temporal trends in carbonaceous aerosols in the United Kingdom, Atmos. Environ., in press, https://doi.org/10.1016/j.apr.2020.09.009.

Jones, A.M., Harrison, R.M., 2005. Interpretation of particulate elemental and organic carbon concentrations at rural, urban and kerbside sites, Atmos. Environ., 39, 7114-7126.

Jones, A.M., Harrison, R.M., Fuller, G., Barratt, B., 2012. A large reduction in airborne particle number concentrations at the time of the introduction of "sulphur free" diesel and the London Low Emission Zone, Atmos. Environ., 50, 129-138.

Kendrick, C.M., Koonce, P., George, L.A., 2015. Diurnal and seasonal variations of NO, NO_2 and $PM_{2.5}$ mass as a function of traffic volumes alongside an urban arterial, Atmos. Environ., 122, 133-141.

Masiol, M., Agostinelli, C., Formenton, G., Tarabotti, E., Pavoni, B., 2014. Thirteen years of air pollution hourly monitoring in a large city: Potential sources, trends, cycles and effects of car-free days, Sci.Tot. Environ., 494-495, 84-96.

Matthaios, V.N., Kramer, L.J., Sommariva, R., Pope, F.D., Bloss, W. J., 2019. Investigation of vehicle cold start primary NO2 emissions inferred from ambient monitoring data in the UK and their implications for urban air quality. *Atmospheric Environment*, *199*, 402 - 414.

Mbengue, S., Fusek, M., Schwarz, J., Vodička, P., Šmejkalová, A.H., Holoubek, I., 2018. Four years of highly time resolved measurements of elemental and organic carbon at a rural background site in Central Europe, Atmos. Environ., 182, 335- 346.

Reche, C., Viana, M., Moreno, T., Querol, X., Alastuey, A., Pey, J., Pandolfi, M., Prévôt, A., Mohr, C., Richard, A., Artiñano, B., Gomez-Moreno, F.J., Cotse, N., 2011. Peculiarities in atmospheric particle number and size-resolved speciation in an urban area in the western Mediterranean: Results from the DAURE campaign, Atmos. Environ., 45, 5282-5293.

Sabaliauskas K., Jeong C.-H., Yao X., Jun Y.-S., Jadidian P., Evans G.J., 2012. Five-year roadside measurements of ultrafine particles in a major Canadian city, Atmos. Environ., 49, 245-256.

Seo, J., Park, D.-S.R., Kim, J.Y., Youn, D., Lim, Y.B., Kim Y., 2018. Effects of meteorology and emissions on urban air quality: a quantitative statistical approach to long-term records (1999-2016) in Seoul, South Korea, Atmos. Chem. Phys., 18, 16121-16137.

Shahid, I., Alvi, M.U., Shahid, M.Z., Alam, K., Chishtie, F., 2018. Source Apportionment of PM10 at an Urban Site of a South Asian Mega City. Aerosol and Air Quality Research, 18, 2498–2509.

Shin, H.J., Roh, S.A., Kim, J.C., Lee, S.J., Kim, Y.P., 2013. Temporal variation of volatile organic compounds and their major emission sources in Seoul, Korea, Environ. Sci. Pollut. Res., 20, 8717-8728.

Sicard, P., Agathokleous, E., De Marco, A., Paoletti, E., Calatayud, V., 2021. Urban population exposure to air pollution in Europe over the last decades. Environmental Sciences Europe, 33, 28. https://doi.org/10.1186/s12302-020-00450-2.

Thorpe, A., Harrison, R.M., 2008. Sources and properties of non-exhaust particulate matter from road traffic: A review, Sci. Tot. Environ., 400, 270-282.

Twigg, M.M., Di Marco, C.F., Leeson, S., van Dijk, N., Jones, M.R., Leith, I.D., Morrison, E., Coyle, M., Proost, R., Peeters, A.N.M., Lemon, E., Frelink, T., Braban, C.F., Nemitz, E., Cape, J.N., 2015. Water soluble aerosols and gases at a UK background site - Part 1: Controls of $PM_{2.5}$ and PM_{10} aerosol composition, Atmos. Chem. Phys., 15, 8131-8145.

Vingarzan, R., 2004. A review of surface ozone background levels and trends, Atmos. Environ., 38, 3431-3442.

von Bismarck-Osten, C., Birmili, W., Ketzel, M., Massling, A., Petäjä, T., Weber, S., 2013. Characterization of parameters influencing the spatio-temporal variability of urban particle number size distributions in four European cities, Atmos. Environ., 77, 415-429.

Vu, T.V., Shi, Z., Cheng, J., Zhang, Q., He, K., Wang, S., Harrison, R.M., 2019. Assessing the impact of clean air action on air quality trends in beijing using a machine learning technique, Atmos. Chem. Phys., 19, 11303-11314.

White, W.H., 2008. Chemical markers for sea salt in IMPROVE aerosol data. Atmospheric Environment, 42, 261–274.

Xue, Q., Jiang, Z., Wang, X., Song, D., Huang, F., Tian, Y., Huang-fu, Y., Feng, Y., 2019. Comparative study of PM10-bound heavy metals and PAHs during six years in a Chinese megacity: Compositions, sources and source specific risks. Ecotoxicology and Environmental Safety, 186, 109740.

Young, D. E., Allan, J. D., Williams, P. I., Green, D. C., Flynn, M. J., Harrison, R. M., Yin, J., Gallagher, M. W., Coe, H., 2015. Investigating the annual behaviour of submicron secondary inorganic and organic aerosols in London. Atmospheric Chemistry and Physics, 15, 6351–6366.

Zhang, R., Ho, K.-F., Cao, J., Han, Z., Zhang, M., Cheng, Y., Lee, S.C., 2009. Organic carbon and elemental carbon associated with PM_{10} in Beijing during spring time, J. Hazard. Mater., 172, 970-977.

Zhao, S., Yu, Y., Yin, D., He, J., Liu, N., Qu, J., Xiao, J., 2016. Annual and diurnal variations of gaseous and particulate pollutants in 31 provincial capital cities based on in situ air quality monitoring data from China National Environmental Monitoring Center, Environ.Int., 86, 92-106.

TABLES LEGENDS:

Table 1: Long-term trend in pollutant concentrations for the period 2009-2018.

Table 2: Roadside Increment of PM at Marylebone Road for the period 2009-2018.

Table 3: Roadside increment (ng m^{-3}) for heavy metal concentrations for the period 2011-2018.

Table 4: Roadside increment (µg m^{-3}) for EC and OC for the period 2010 – 2018 at Marylebone Road.

Table 5: A review of some studies profiling urban air quality status

FIGURE LEGENDS:

Figure 1: Diurnal, weekly and monthly time series plot for regulated pollutants at Marylebone Road.

Figure 2: 1:1 Scatterplot for BC and $PM_{2.5}$ by wind direction (right scale, degrees).

Figure 3: Diurnal, weekly and monthly time series plot for VOCs at Marylebone Road.

Figure 4a: Yearly mean metal concentrations in PM_{10} at Marylebone Road.

Figure 4b: Yearly mean metal concentrations in PM_{10} without Fe at Marylebone Road.

Figure 5: 1:1 Scatter plot for PM_{10} for both LMR and LNK for the northerly wind direction

Figure 6: Polar plot for nitrogen oxides showing significance of wind parameters for pollutant dispersion. The direction from the centre of the plot shows the wind direction above the canyon and the distance from the centre is the wind speed (scale in metres per second).

Figure 7: Polar plot for PM fractions showing significance of wind conditions to pollutant dispersion.

Figure 8: Polar plot of the robust slope between $PM_{2.5}$ and BC for 2013 at London, Marylebone Road.

Figure 9: Polar plot for EC (left) and OC showing the influence of wind direction and speed.

Figure 10: Long-term trend in average monthly total particle number count for London, Marylebone Road.

Figure 11: Diurnal, weekday and monthly variation in total particle count for London Marylebone Road.

Figure 12: Plot of dependence of particle count on wind conditions.

Figure 13: The average particle number size distribution curve for data for the period 2010-2018.

Table 1: Long-term trend in pollutant concentrations for the period 2009-2018.

Site name	Site type	Parameter (%/year)								
		NO_x	NO_2	O_3	SO_2	CO	$PM_{2.5}$	PM_c	PM_{10}	Period
London Marylebone Road	Urban Traffic	-1.22*	-2.10***	0.63	-0.42	-5.47***	-4.00***	-3.43***	-3.93***	2009 - 2018

Note: the asterisk relates to the statistical significance of the trend estimate: $p < 0.001 = ***$, $p < 0.01 = **$, $p < 0.05 = *$ and $p < 0.1 = +$

Table 2: Roadside Increment of PM at Marylebone Road for the period 2009-2018.

	2009	**2010**	**2011**	**2012**	**2013**	**2014**	**2015**	**2016**	**2017**	**2018**
Daily Data										
ΔPM_{10} ($\mu g/m^3$)	16.7	13.6	16.1	12.7	10.2	10.1	10.1	9.9	NA	NA
$\Delta PM_{2.5}$ ($\mu g/m^3$)	7.0	8.1	9.0	8.1	5.8	5.9	5.2	4.5	NA	NA
ΔPM_c ($\mu g/m^3$)	9.7	5.6	7.1	4.6	4.4	4.2	4.9	5.3	NA	NA
Hourly Data										
ΔPM_{10} ($\mu g/m^3$)	14.2	13.0	14.8	10.4	8.6	4.1	4.3	6.1	7.3	9.9
$\Delta PM_{2.5}$ ($\mu g/m^3$)	8.1	6.6	7.6	6.9	5.0	2.1	4.8	3.8	3.7	6.6
ΔPM_c ($\mu g/m^3$)	6.1	6.4	7.2	3.4	3.5	2.0	-0.4	2.4	3.6	3.3

Table 3: Roadside increment (ng m^{-3}) for heavy metal concentrations for the period 2011-2018.

Metals	**Year**							
	2011	**2012**	**2013**	**2014**	**2015**	**2016**	**2017**	**2018**
As	0.127	0.348	0.011	0.136	0.092	0.226	0.123	0.069
Cd	0.072	0.014	0.013	0.038	0.027	0.029	0.035	0.030
Cu	67.6	54.6	44.9	46.0	41.7	38.0	48.3	39.2
Fe	1354	1208	1042	1133	1103	1069	1469	1153
Mn	10.8	9.90	8.05	8.61	8.39	8.35	11.9	8.94
Ni	1.33	1.45	0.85	0.62	0.73	0.91	0.99	0.77
Pb	0.102	2.86	-0.179	-0.626	-0.147	3.303	0.180	0.150
V	0.188	0.503	0.149	0.270	0.323	0.294	0.336	0.165
Zn	17.9	30.4	9.34	9.66	11.6	13.3	20.6	16.6

Table 4: Roadside increment (µg m^{-3}) for EC and OC for the period 2010 – 2018 at Marylebone Road.

	2010	2011	2012	2013	2014	2015	2016	2017	2018
ΔEC	5.42	5.89	5.23	3.67	3.89	3.17	2.73	2.50	1.83
ΔOC	2.64	3.63	3.24	2.47	2.20	2.44	1.90	2.18	2.10

Table 5: A review of some studies profiling urban air quality status

No	Outcome	Author and Location
1	Investigation of regulated gas phase pollutants and VOCs over a 13-year period (2000-2013) in the Po Valley of Italy. The main emission sources in the region included vehicular, industrial, domestic heating, airport and harbour. The long-term trend analysis of the pollutants showed decreases in the mean concentration of CO, SO_2 and the VOCs, but no significant change in the level of the oxides of nitrogen, while O_3 levels showed a slight increase. The declining trend in some of the pollutants over the period was attributed to a reduction in industries, use of better grade fuel and technological improvement in the emission standards for road vehicles. All of the pollutants showed a seasonal cycle, except SO_2. This unexpected behaviour of SO_2 was due to a very high rate of oxidation i.e. shorter atmospheric residence time. Ozone showed maximum concentrations during the warmest periods while CO, the oxides of nitrogen, VOCs and PM_{10} produce their highest concentrations in winter, due to an increase in domestic emissions and stable atmospheric conditions. O_3 and SO_2 showed a maximum daily concentration around midday with a greater amplitude in summer. The normal twin peaks corresponding to the morning and evening traffic rush hours were seen for CO, NO, NO_2, NO_x, PM_{10} and VOCs. This is a coastal location and the local sea breeze circulation influences the distribution of the pollutants during daytime. The weekday/weekend cycles showed higher weekday concentration of CO, VOCs and the oxides of nitrogen with the reverse observed for ozone. SO_2 and PM_{10} exhibited a similar pattern throughout the weekdays and weekends.	Masiol et al., 2014 Po Valley, Italy
2	A report of hourly data for $PM_{2.5}$ and O_3 for the period 2006 – 2015 from several stations in Tehran with temporal changes investigated using the Mann-Kendall trend test. The earlier years showed an almost constant annual mean $PM_{2.5}$ concentration, but a significant decline occurred from 2010 to 2015 at a rate of 1.17 µg m^{-3}/year. For O_3, there was an initial increase in yearly mean from 2006 – 2008 followed by a significant decline (3.39 µg m^{-3}) from 2008 to 2015, with 2015 giving the lowest annual mean concentration. The data show a bimodal diurnal peak for	Faridi et al., 2018 Tehran, Iran

	$PM_{2.5}$ corresponding to periods with significant anthropogenic emissions. The first peak occurred around 07:00 to 09:00 corresponding to heavy road traffic in the morning rush hour. The second peak occurred around midnight and beyond correlating with a second traffic rush hour (including heavy-duty diesel vehicles) and construction and demolition activities. Analysis of $PM_{2.5}$ for the different days of the week showed statistically significant higher values during the weekdays over the weekend (Friday). The O_3 values showed maximum concentrations at around 3:00 pm and were higher over the weekends than the weekdays. This profile points to the significant contribution of human activities, especially vehicular traffic to poor air quality. There was a seasonal pattern in the concentration of $PM_{2.5}$ with maximum levels in winter and summer months. The high summer PM concentration is because of the Middle East dust events especially in summer, and the winter high is due to stable meteorological conditions (i.e. low mixing depth, low temperatures and weak wind). O_3 also showed seasonal variability with maximum monthly concentrations recorded in July due to enhanced photochemical reactions.	
3	Air pollution in major Chinese cities was investigated for close to a period of one year by monitoring regulated particulate matter and gas phase pollutants (CO, NO_2, O_3, SO_2, $PM_{2.5}$ and PM_{10}). There was a winter maximum for all the criteria pollutants, except for ozone. This maximum concentration results from increased emissions and meteorological conditions that limit dispersion of pollutants. Coal combustion and residential heating are major contributors to the increased emissions during wintertime. O_3 gave a summer maximum and a winter minimum. The diurnal variation of O_3 had a maximum during daytime with the other pollutants giving the lowest concentrations at this time because of higher wind speeds and an increased boundary layer height. Generally, the particulate matter fractions, NO_2 and CO produced peaks corresponding to the morning and evening traffic rush hours, while SO_2 had a single peak around 11:00 am. Vu et al., (2019) report five year (2013-2017) trends in pollutants averaged across sites in the Beijing area, and corrected for the effects of weather variations. Steady falls in concentrations of all measured pollutants apart from ozone are attributable to an air quality action plan.	Zhao et al., 2016; Vu et al., 2019 Chinese cities
4	Analysis of long-term real time air quality monitoring data (1996-2008) from a background site in central London which showed a general downward trend for several pollutants except ozone, which rose at a steady rate. The downward trends shown by the pollutants were however not uniform and occurred at different rates. For instance, CO and NO showed a close pattern in their trend analysis with a maximum observed around 1996-1998, and a steady decline afterwards, whereas SO_2 showed minimal fluctuations, and the concentration remained nearly constant. PM_{10} also showed a pattern that appeared constant	Bigi and Harrison, 2010 London, England

	throughout the period of investigation. Ozone showed the greatest seasonal variability with a maximum in May and a minimum in December, with this pattern influenced by background concentrations. CO, NO and NO_2 showed a winter maximum, and minimum values in June and July. PM_{10} showed little seasonal variation. The traffic related pollutants showed a bimodal peak corresponding to the morning and evening traffic rush hour peaks resulting from high traffic volumes and poor dispersion, with PM_{10} and particle count showing lesser amplitudes. Ozone showed a single peak at about 16:00 hrs due to less scavenging of the pollutant in the afternoon and more mixing from aloft in a deeper boundary layer. On average, all the pollutants gave their maximum concentrations in the weekdays and minimum over the weekends, with the reverse observed for O_3.	
5	Hourly data for nitrogen oxides and particulate matter size fractions for Paris (44 sites) and London (130 sites) for the period 2005 – 2016 were investigated. The annual mean concentration of NO_2 exceeded the European Limit Value across all network especially for the roadside locations for both cities with background locations in Paris achieving compliance by 2016. The Limit Value for PM_{10} is mostly attained across the networks in both cities, attributed to controls by the Euro 5 (light duty) and Euro V (heavy duty) standards. There were overall significant declining trends for the pollutants in both cities with the rates higher at the background sites. In 2005 – 2009, there was an increase in roadside increment in NO_2 due to an increase in the proportion of diesel vehicles, and with the introduction of the Euro V standard, a significant decline in the roadside increment of the pollutant was recorded between 2010 - 2016. However, for the PM_{10}, the roadside increment declined for both periods of measurement with London (especially inner London) showing a greater decrease than Paris. While the roadside increment in $PM_{2.5}$ show a significant downward trend in Paris, it was mostly non-significant in the case of London. The study showed a significant gain made by policies in reducing particulate matter emissions but not as expected in the case of NO_2.	Font et al., 2019 Paris, France and London. England
6	The chemical composition of non-refractory PM_1 (by ACSM) and BC (Multichannel Aethalometer) were investigated for Delhi to determine temporal variation in aerosol composition. There was seasonal variability in the PM mass concentration (NR-PM_1 and C-PM_1 = NR-PM_1 + BC), with winter levels giving the highest concentration. The winter values were up to 4 times higher than the warmer periods. There was diurnal variation in the concentrations of the PM and components, with the greatest diurnal swings occurring in winter. Generally, the peak periods occurred in the morning and late evening, with lowest concentrations between 15:00 – 16:00 hrs. The organic component at highest contributed about 50% to C-PM_1. Ammonium contributed most to the inorganic component balancing the anions, however, chloride exhibited the greatest	Gani et al., 2019 Delhi, India

	seasonal variability of all these species (winter concentrations up to 20 times the summer concentrations) and with highest global concentrations. Nitrate and sulphate also showed seasonal variation with the nitrate showing the least seasonal and diurnal variability and being the only species that gave elevated levels in the warmer period during daytime. BC concentrations were lower during the day and peaked at night due to high truck traffic passing close to the sampling location at night. The average BC concentration was higher in the winter than summer but contributed 6.4% of the total mass concentration of C-PM_1 in winter as compared to 14% in the summer	
7	The study analysed aerosol samples for PM_{10}-bound PAHs and heavy metals in Chengdu (China) for a period of 6 years (with ions, OC and EC analysed for source apportionment), with the sampling period divided into wet (Jun - Oct) and dry (Jan – Apr and Dec.) periods. The mean PM_{10} concentration was higher for the dry period, but both periods exceeded the 70µg m^{-3} limit set by the regulatory body in China. The high PM_{10} concentration in the dry period was due to stable weather conditions, low precipitation and higher coal usage. The mean concentration for the 16 PAHs (from coal combustion and vehicle exhaust) also show statistically significant higher values in the dry period compared to the wet. For the heavy metals, As and Ni were higher in the wet period whereas Cr, Co, Cd and Pb were higher in the dry period. However, there was greater variability exhibited by the PAHs with PM_{10} than the heavy metals for the period under investigation. A PMF model analysis for PM_{10} examined 18 elements, 3 ions, OC, EC and 16 PAHs. The first two factors accounted mainly for gasoline and diesel combustion. Coal combustion, industrial sources, crustal dust and secondary aerosol formation were the other sources identified by the model. The percentage contributions of gasoline and diesel combustion were similar in the dry and wet periods, whereas, coal combustion, crustal dust and secondary aerosol formation gave a higher contribution in the dry period (winter) and the contribution by industrial sources was maximised in the wet period.	Xue et al., 2019 Chengdu, China
8	Trace metal analysis of the PM_{10} fraction using an ICP-AES spectrometer was conducted for aerosol samples collected in Karachi (Pakistan) and PMF analysis conducted for source apportionment. The average PM_{10} concentration recorded of 438µg m^{-3} is comparable to levels reported elsewhere in Asia and some other cities in Pakistan. The mean concentrations of trace metals were categorised into groups: Ca, Al and Fe (13730 – 57260ng m^{-3}); Mg and S (7350ng m^{-3} and 6390ng m^{-3} respectively); Zn, P, Cu, Pb, Mn, Ti, Sr and Ba (220 – 830ng m^{-3}) and Cr, Ni, Se (50ng m^{-3}, 20ng m^{-3} and 10ng m^{-3} respectively). The PMF analysis identified biomass burning, coal combustion, resuspended dust, vehicular emissions and industrial dust as the contributors to the PM_{10} mass concentrations.	Shahid et al., 2018 Karachi, Pakistan

1027

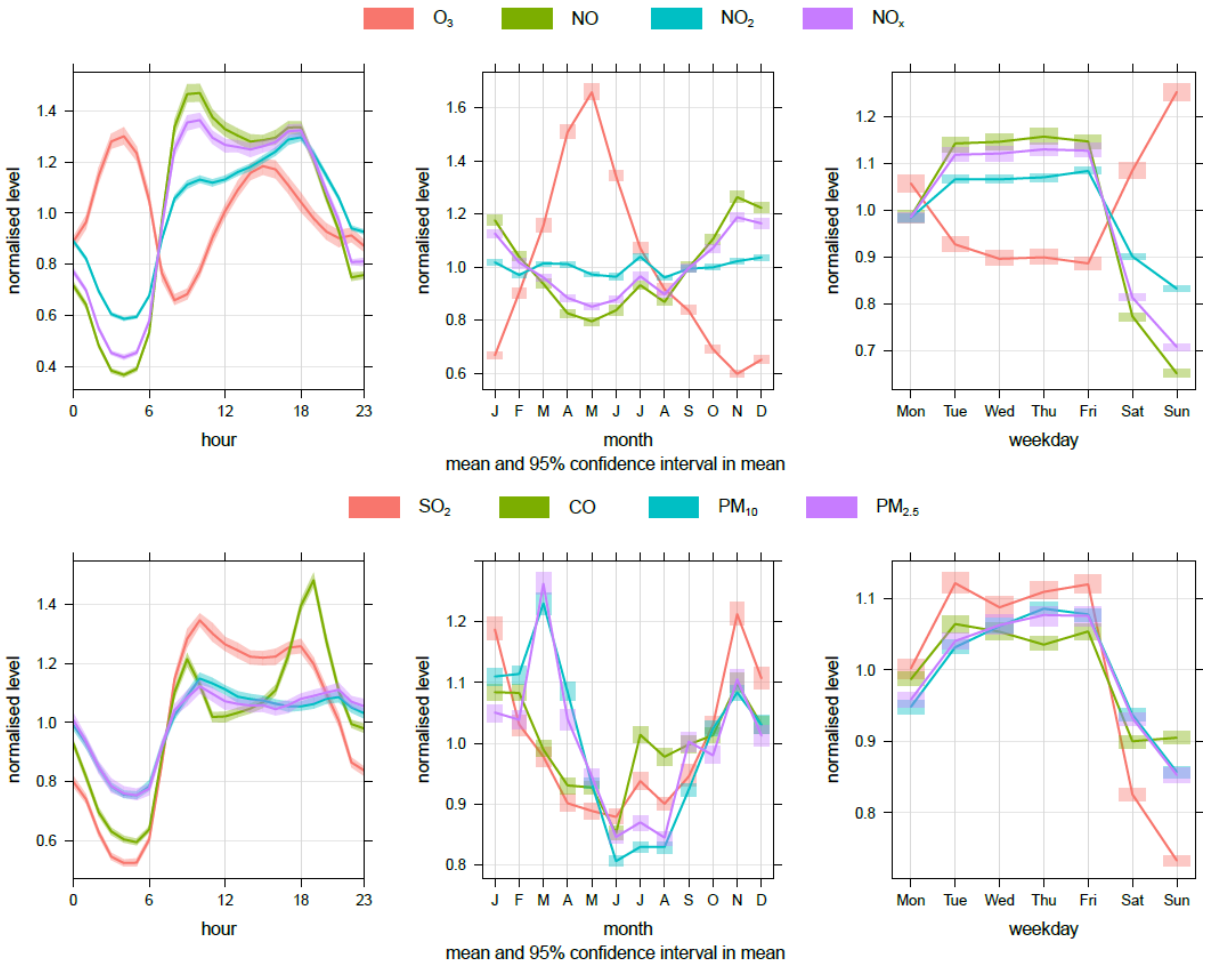

Figure 1: Diurnal, weekly and monthly time series plot for regulated pollutants at Marylebone Road.

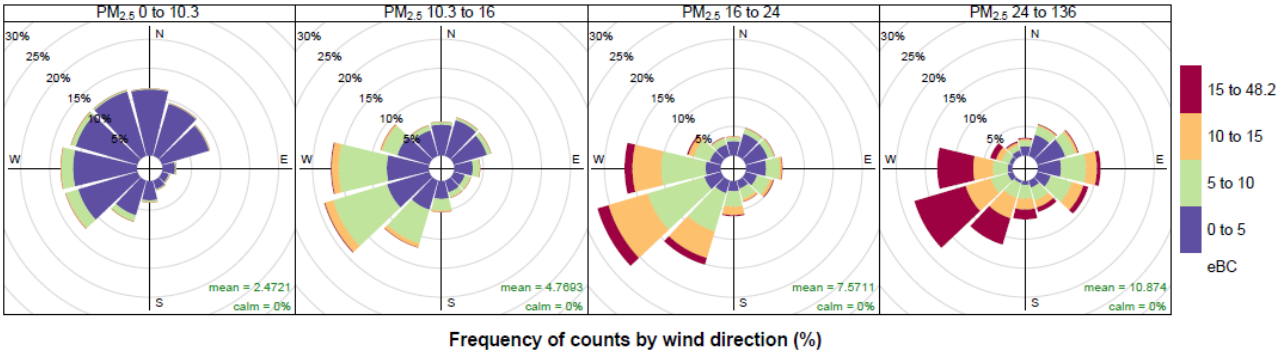

Figure 2: eBC pollution rose according to $PM_{2.5}$ concentration range.

1039
1040

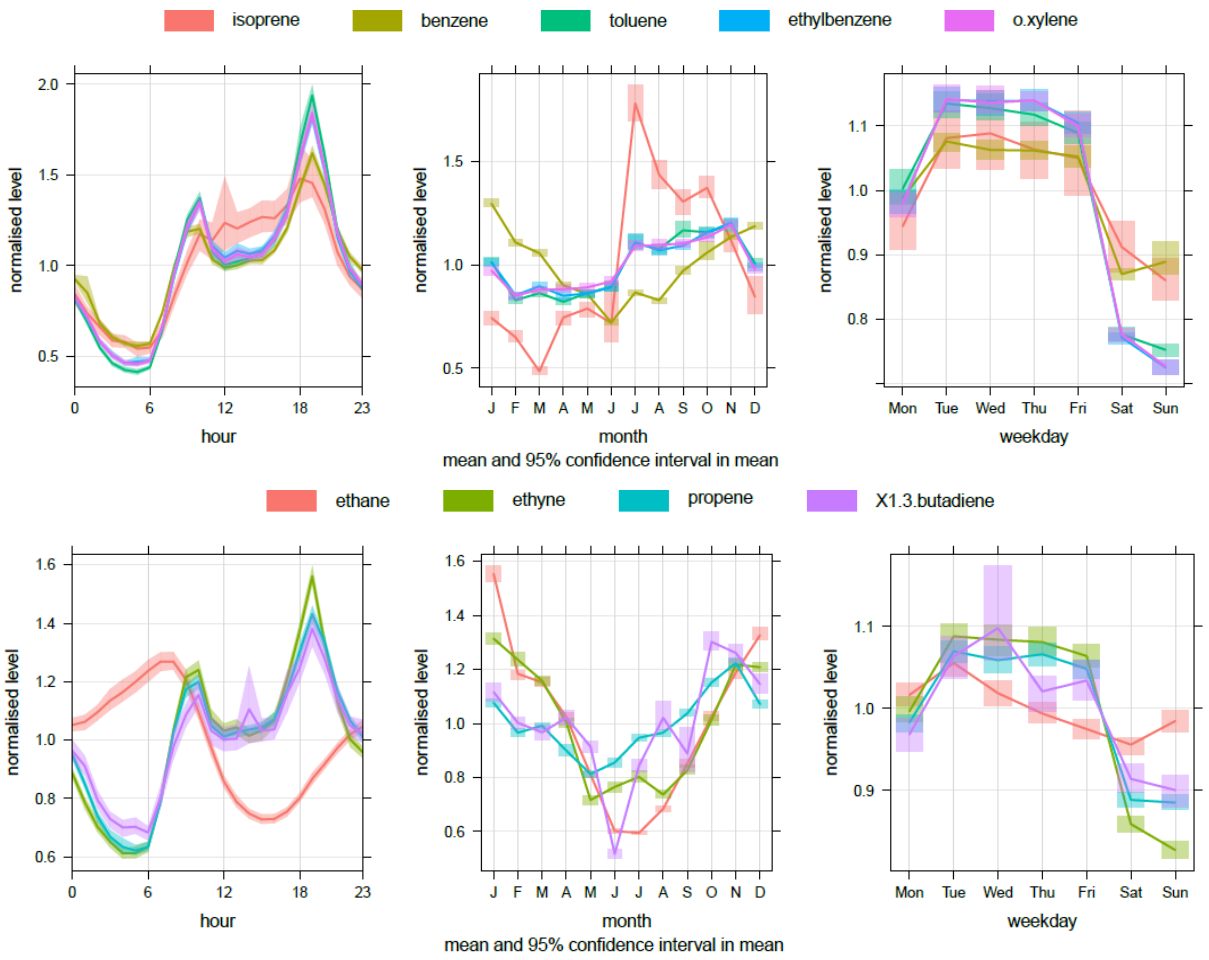

Figure 3: Diurnal, weekly and monthly time series plot for VOCs at Marylebone Road.

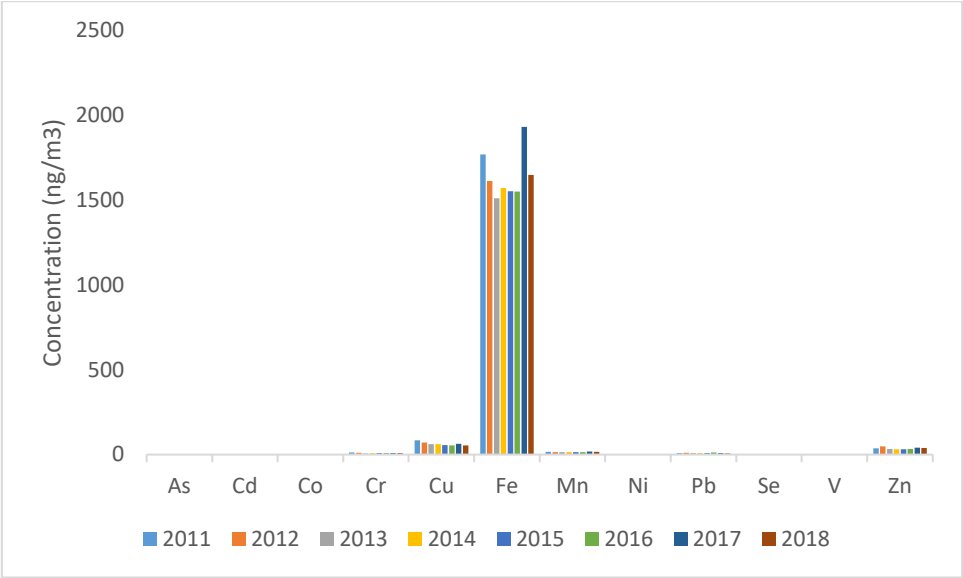

Figure 4a: Yearly mean metal concentrations in PM_{10} at Marylebone Road.

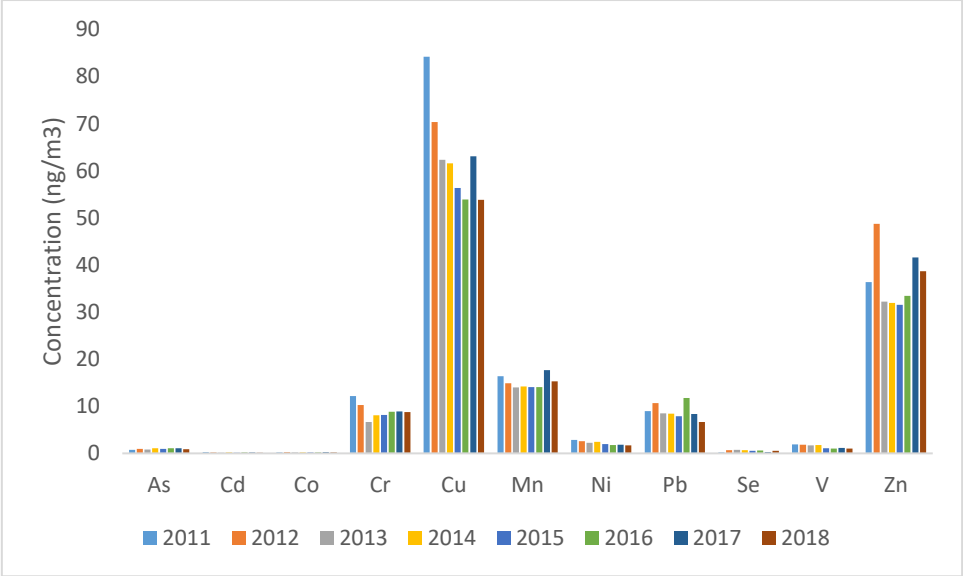

Figure 4b: Yearly mean metal concentrations in PM_{10} without Fe at Marylebone Road.

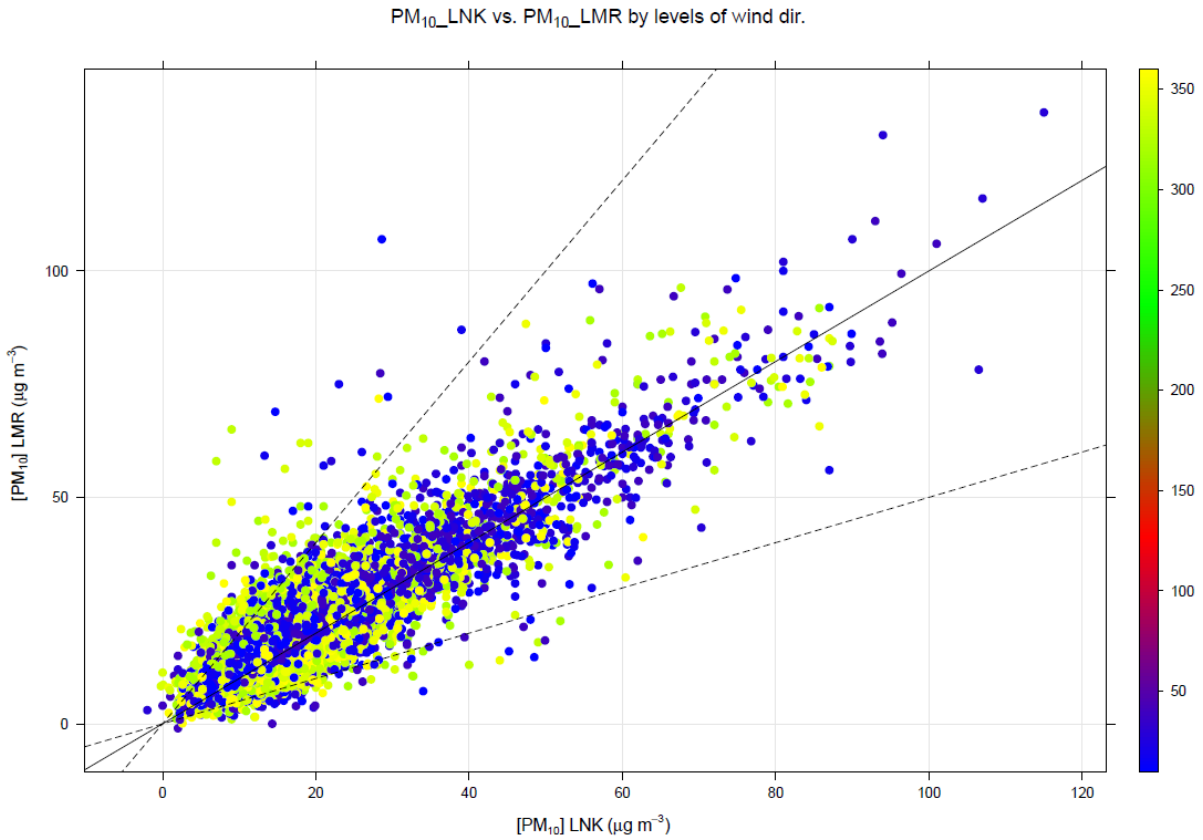

Figure 5: 1:1 Scatter plot for PM_{10} for both London Marylebone Road (LMR) and London North Kensington (LNK) for the northerly wind direction

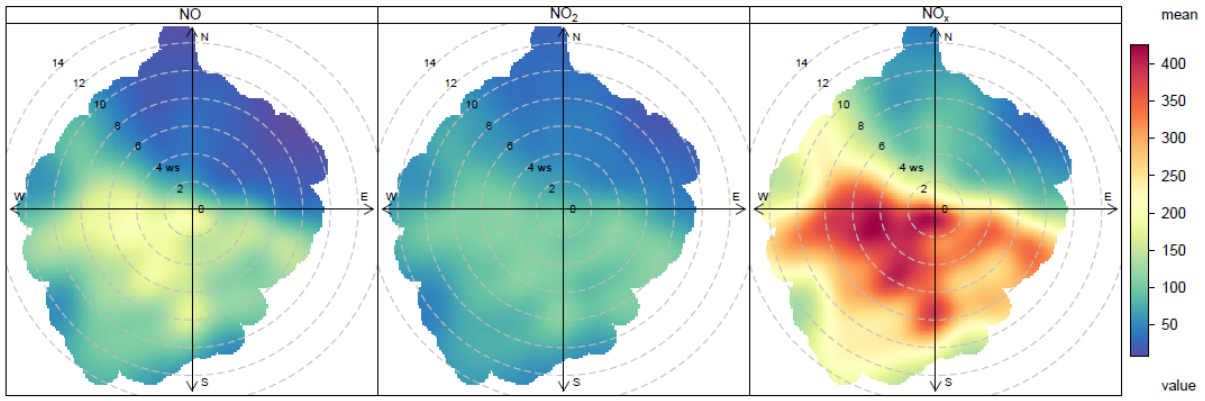

Figure 6: Polar plot for nitrogen oxides showing significance of wind parameters for pollutant dispersion. The direction from the centre of the plot shows the wind direction above the canyon and the distance from the centre is the wind speed (scale in metres per second).

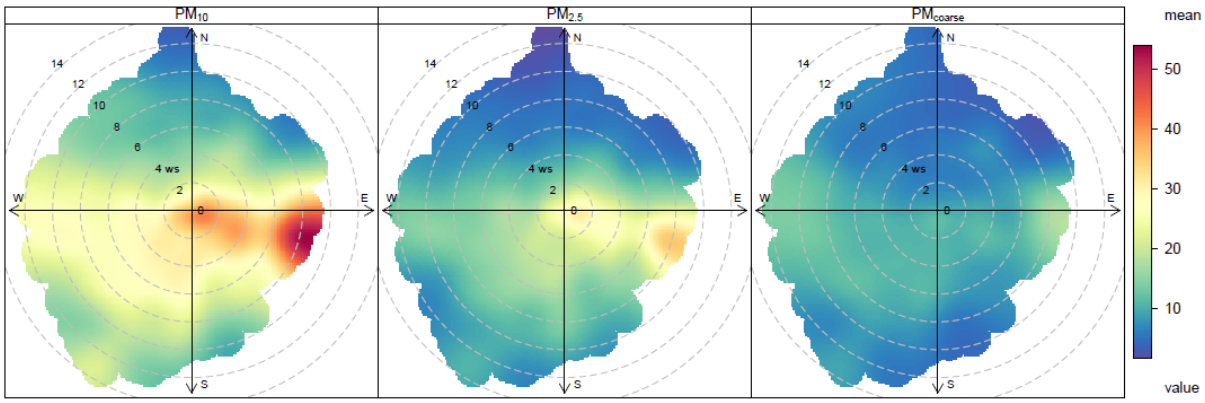

Figure 7: Polar plot for PM fractions showing significance of wind conditions to pollutant dispersion.

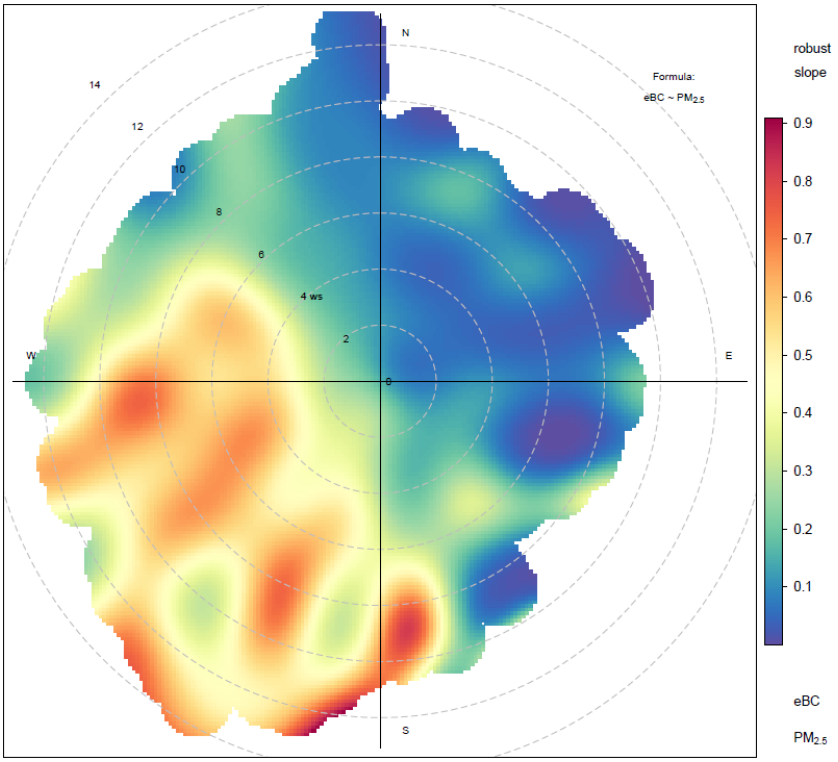

Figure 8: Polar plot of the robust slope between $PM_{2.5}$ and BC at London, Marylebone Road.

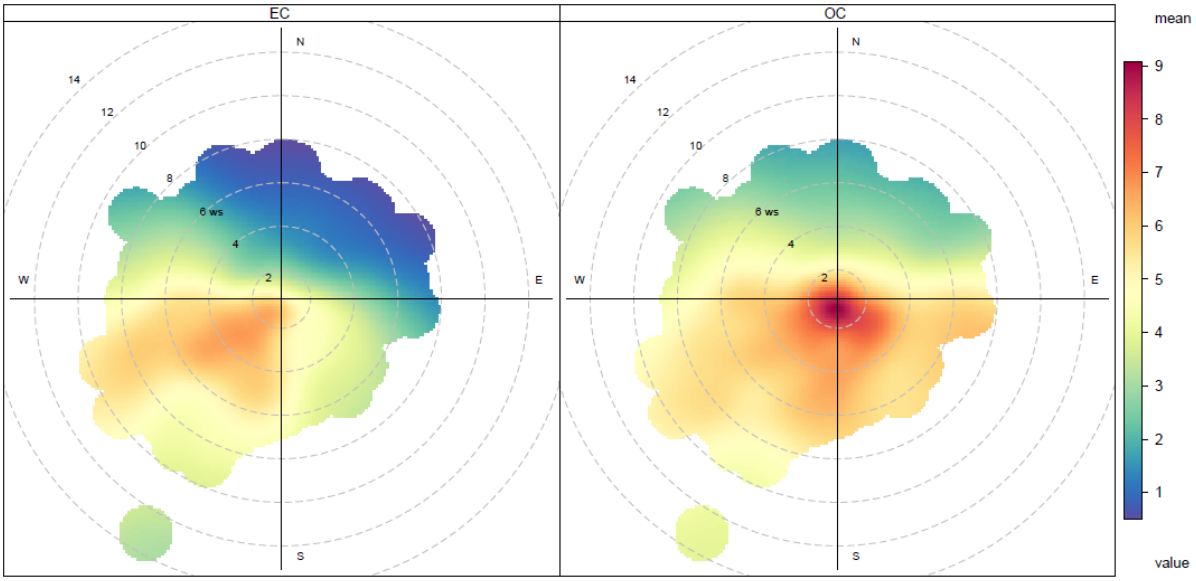

Figure 9: Polar plot for EC (left) and OC showing the influence of wind direction and speed.

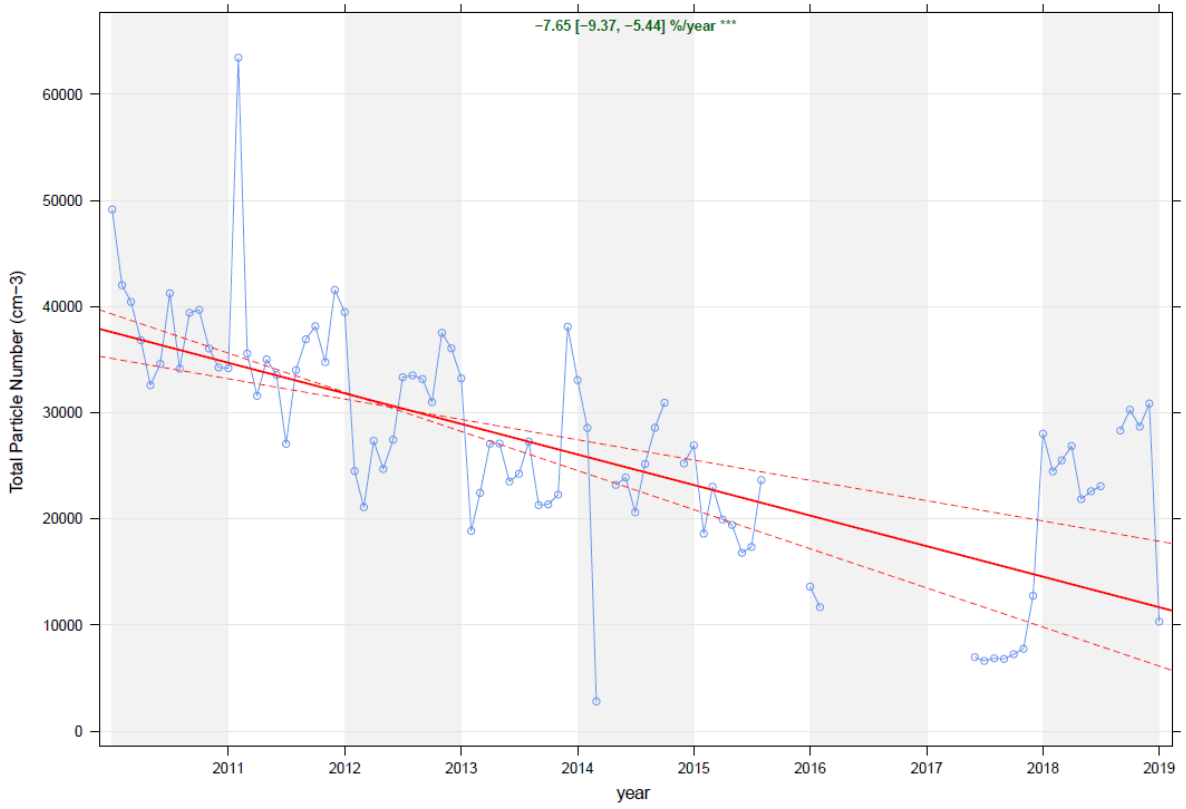

Figure 10: Long-term trend in average monthly total particle number count for London, Marylebone Road.

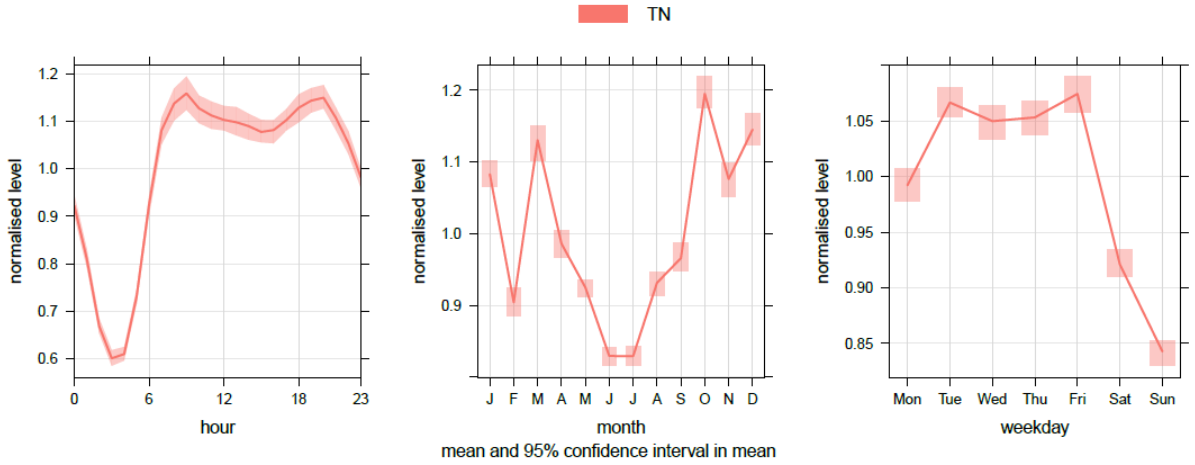

Figure 11: Diurnal, weekday and monthly variation in total particle count for London Marylebone Road.

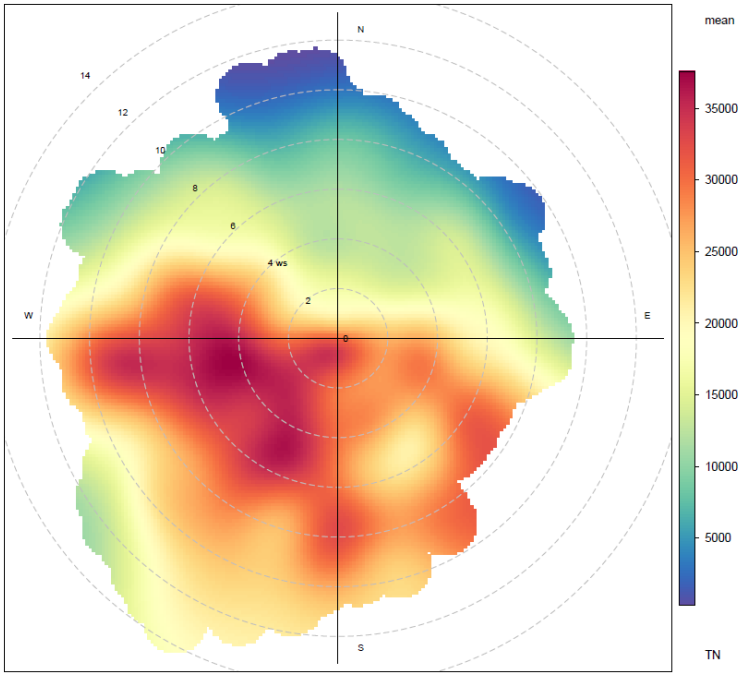

Figure 12: Plot of dependence of particle count on wind conditions.

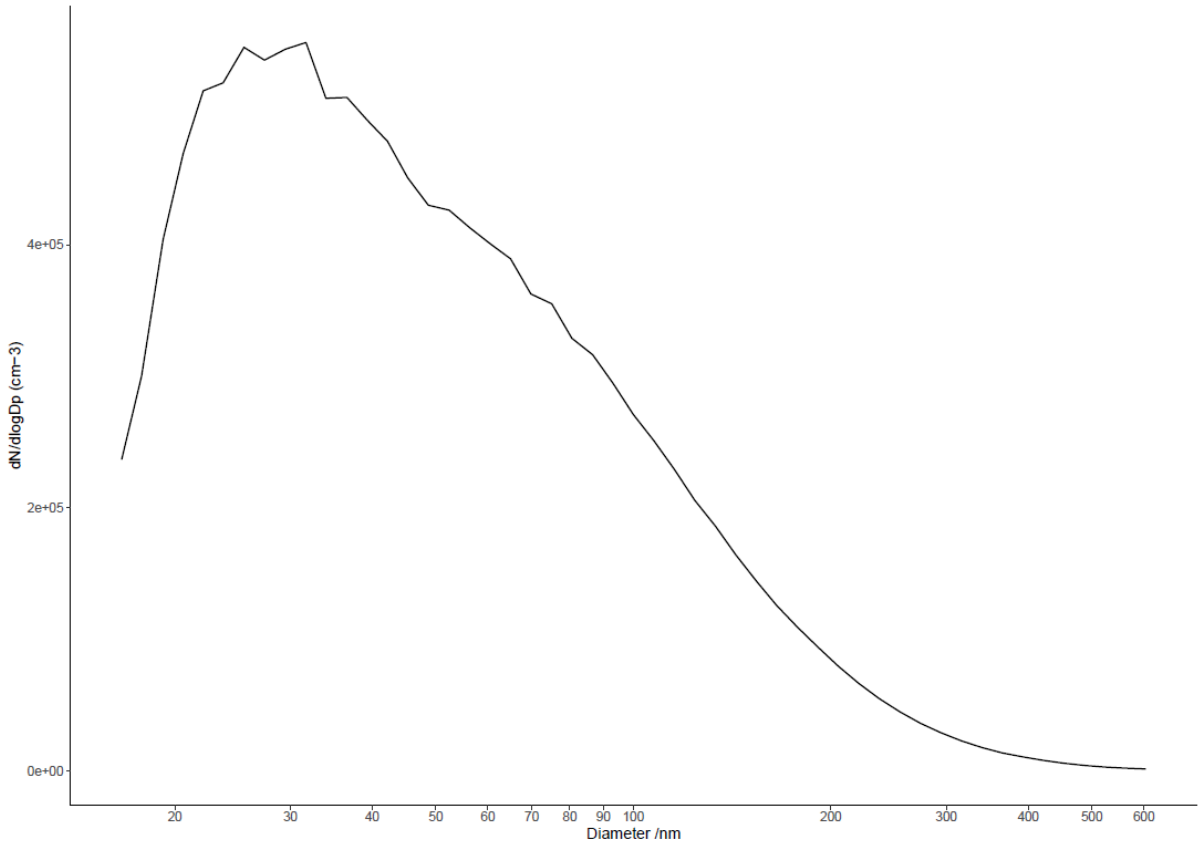

Figure 13: The average particle number size distribution curve for data for the period 2010-2018.